

GEOLOGICAL SURVEY OF CANADA

OPEN FILE 2749

This document was produced
by scanning the original publication.

Ce document a été produit par
numérisation de la publication originale.

**Mineralogy and chemical variations of
sulphides from the Crystal Lake Intrusion,
Thunder Bay, Ontario**

E.H. Cogulu

1993



NODA • EDNO



CANADA
ONTARIO

Northern Ontario
Development Agreement

Entente de développement
du nord de l'Ontario

Minerals • Minéraux

Canada

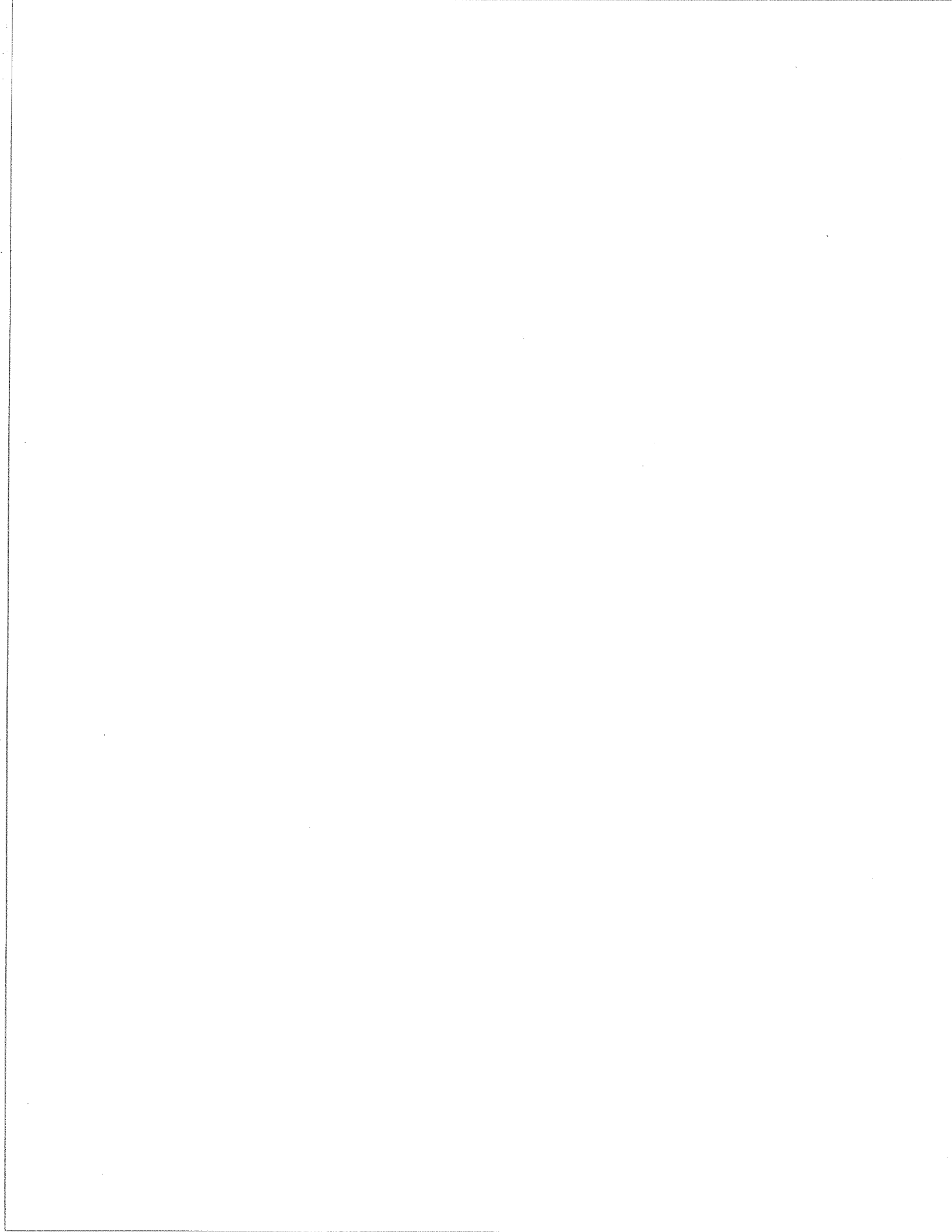
Contribution to Canada-Ontario Subsidiary Agreement on Northern Ontario Development (1991-1995), a subsidiary agreement under the Economic and Regional Development Agreement. Project funded by the Geological Survey of Canada.

Contribution à l'Entente auxiliaire Canada-Ontario de développement du nord de l'Ontario (1991-1995), entente auxiliaire négociée en vertu de l'Entente de développement économique et régional. Ce projet a été financé par la Commission géologique du Canada.

**MINERALOGY AND CHEMICAL VARIATIONS
OF SULPHIDES FROM THE CRYSTAL LAKE
INTRUSION, THUNDER BAY, ONTARIO**

ERSEN H. COGULU

Report submitted under the terms
of DSS contract no. 34SZ.23233-7-760
Canada-Ontario Mineral Development Agreement



ABSTRACT

The Crystal Lake intrusion located 47 km southwest Thunder Bay-Ontario is a layered intrusion related to the Duluth Complex, Minnesota. It hosts the Great Lakes Nickel (GLN) Cu-Ni deposit in its unlayered lower and basal zones, and contains Platinum Group Element (PGE) and chrome spinel mineralization in the overlying cyclic layered zone. Sulphide disseminations are mainly concentrated in the keel zone of the canoe-shaped layering which plunges 15-20° to the east. Sulphides form interstitial and included grains and droplets. Some sulphide blebs display chalcopyrite tops and pyrrhotite bottoms (polarity textured blebs), apparently a result of fractional crystallization of the sulphide liquid.

Pyrrhotite, chalcopyrite, cubanite and pentlandite are the main sulphides. Niccolite, maucherite, native Bi, mackinawite, bornite, millerite, nickeloan pyrite and marcassite occur in accessory amounts. Chalcopyrite and cubanite are dominant in the cyclic units while pyrrhotite is the main sulphide in the lower zones. Monoclinic pyrrhotite is the dominant iron sulphide in the basal and contact zones. Electron microprobe analyses of pentlandite reveal systematic compositional variations in Ni and Co contents. Pentlandites coexisting with troilite have the lowest Ni content, while those associated with hexagonal pyrrhotite, monoclinic pyrrhotite, and chalcopyrite respectively, have progressively greater Ni contents. Cobalt content of pentlandites increases with depth in the intrusion and attains 7.0 wt% in the basal-contact zones as well as in xenoliths.

Textural and compositional evidence indicates that the Crystal Lake gabbroic magma was contaminated by assimilation of sedimentary xenoliths, and by devolatilization of contact rocks. Sulphur, iron, cobalt, silica and volatiles were added to the magma and played key roles during the sulphide mineralization. Cyclic zone sulphides are not contaminated, but they are more closely associated with volatiles than those of the lower zones. Cubanite crystallization is related to the resorption of early pyrrhotite by chalcopyrite. An immiscible sulphide liquid separated from the silicate magma and gave rise to early iron-rich monosulphide solid solution (mss). Later, copper-rich intermediate solid solution (iss) and volatiles were segregated by fractional crystallization.

INTRODUCTION

The Crystal Lake intrusion is located approximately 47 km southwest of Thunder Bay, Ontario. It hosts the Great Lakes Nickel deposit which has been the focus of exploration interest for several mining companies since the 1960's.

Extensive diamond drilling was carried out during the period 1965 to 1974 to explore the Cu-Ni sulphide mineralization. The first description of sulphides was given by Mainwaring (1968). Reeve (1969) described the petrography of the intrusion, and Geul (1970) the general geology of the area. Mainwaring and Watkinson (1981) studied the distribution and composition of chromite in the intrusion. Cogulu (1985) recognised the presence of anomalous PGE in the cyclic zone above the Cu-Ni mineralized zone. Eckstrand and Cogulu (1986) demonstrated that these two zones represent distinct populations of sulphides on the basis of sulphur isotope and Se/S ratios.

The purpose of this paper is to present detailed mineralogical and chemical characteristics of the sulphides, compare them with those of the Duluth Complex, Minnesota, and offer a tentative interpretation.

SAMPLING AND ANALYTICAL METHODS

200 samples were collected from outcrop and drill core. Locations of samples are shown in Fig.1. 150 polished thin sections were studied with a polarizing microscope using transmitted and reflected light.

250 mineral analyses were carried out on a Materials Analysis Company (MAC) electron microprobe equipped with a Kevex energy dispersive spectrometer at the Geological Survey of Canada, Ottawa. Operating conditions were 20 KV acceleration voltage, specimen current of 10 mA, counting time of 100 seconds. Pyrrhotite samples were analysed by XRD camera to determine the structural phase.

GEOLOGICAL SETTING

The Crystal Lake region is situated on the upfaulted northern limb of the Lake Superior Syncline that originated in the late Precambrian (Chase and Gilmer, 1973; Geul, 1970; Davidson Jr., 1982; Franklin et al, 1982). The study area is underlain in large part by sediments of the Rove Formation which represent the northern portion of an Aphebian sedimentary basin. These strata, which consist mainly of argillite, shale and greywacke, were invaded along the Keweenawan Rift zone by volcanic and intrusive rocks of Helikian age. Four groups of Keweenawan intrusive rocks are

distinguished: Logan sills, Pigeon River dikes, Crystal Lake gabbro, and late mafics and granophyres.

The Crystal Lake intrusion outcrops as a "Y" shaped body. Its northern arm is about 750 m wide and extends for about 5.5 km in a west-northwest direction (Fig.1). It is this northern arm that has been most thoroughly explored, and that forms the basis for the present study. The southern arm trends north-easterly, parallel to the Pigeon River dikes, and extends for about 2 km.

The northern arm has canoe-shaped layering which plunges gently (15-20°) toward the east. It comprises four main zones in descending stratigraphic order as follows: 1) the **Upper Zone** consists of alternating layers of olivine gabbro, troctolite, and anorthositic gabbro. It is barren of sulphides. 2) The **Cyclic Zone** is a distinctive layered sequence about 40 m thick. It contains four magmatic cycles, each exhibiting chrome spinel concentrations in olivine-rich adcumulates overlain by anorthositic gabbros. Sparse sulphides are sporadically disseminated throughout the cycles. 3) The **Lower Unlayered Zone (LUZ)** hosts the disseminated Cu-Ni mineralization that is known as the Great Lakes Nickel deposit. This zone is made up of massive gabbro which is characterized by highly variable modal compositions, and by textures ranging from fine grained to pegmatitic. 4) The **Basal Zone** is also mineralized and consists of fine grained gabbros and mixed contact rocks containing abundant sedimentary xenoliths. Footwall sediments were transformed into hornfels adjacent to their contact with the intrusion. Sulphides form droplets and massive bodies within both basal and contact zones. Felsic materials forming anastomosing veins are common in contact gabbros and hornfels.

SULPHIDE OCCURENCES AND DISTRIBUTION

In the northern arm of the Crystal Lake intrusion, sulphide mineralization occurs in the Basal, Lower Unlayered (LUZ), and Cyclic Zones. Two types of mineralization are distinguished: massive, and disseminated. Massive ore occurs in the Basal Zone. It forms irregular masses or lenses which may locally attain 1 m in thickness.

The disseminated mineralization occurs mainly in the Lower Unlayered Zone (LUZ), and is concentrated in the central portion between the north and south margins of this basin shaped layer. It forms discontinuous zones within the LUZ which dip generally eastward, parallel to the plunge of the intrusion. The disseminated sulphides form polygonal grains or blebs ranging in size from a fraction of a mm to a few cm. The grains tend to be polyhedral whereas the blebs are irregular or drop-like in shape, and occur also in sedimentary xenoliths. The

sulphide grains generally consist of two or more sulphides, though single phase grains of chalcopyrite, pyrrhotite or pentlandite occur locally.

Two distinct populations of sulphides are recognizable based on mineral assemblages, and on compositional and textural characteristics of the sulphides. The first population occurs in the Lower Unlayered and Basal Zones. The pyrrhotite is the major phase and constitutes about 70-80% of the sulphides; it is rimmed by other sulphides in lesser proportions. However, monoclinic pyrrhotite increases in amount toward the base of the intrusion, and the basal and contact zone sulphides contain the highest proportion of this phase.

The second population occurs in the Cyclic Zone. Chalcopyrite and cubanite are the two main phases and constitute in general 2/3 of the ore. Pyrrhotite as both hexagonal and monoclinic phases occurs in lesser proportions. Troilite is observed locally in fine grained olivine cumulates.

Pentlandite exhibits systematic compositional characteristics in each population. Cobalt content of pentlandite in the Cyclic Zone is low, always less than 1 wt%. Co content increases with depth in the intrusion. Pentlandite in the Basal and contact zone contains up to 6-7 wt% Co. The Ni content of pentlandite depends upon the co-existing sulphides. Nickel in pentlandite increases corresponding to the following sequence of coexisting minerals: troilite, hexagonal pyrrhotite, monoclinic pyrrhotite, and chalcopyrite. Fig. 3. The assemblage monoclinic pyrrhotite-pentlandite is dominant in the lower mineralized zone, and the pentlandites of this zone are in general richer in nickel than those of the cyclic zone.

A- SULPHIDE MINERALS.

The main sulphide minerals in order of importance are pyrrhotite, chalcopyrite, cubanite and pentlandite. Accessory sulphides are troilite, niccolite, maucherite, millerite, violarite, mackinawite, bornite, sphalerite, nickeloan pyrite, pyrite and marcasite. Representative compositions of the major and minor sulphides are given in Tables 1 to 11.

PYRRHOTITE is the most abundant sulphide and constitutes on average 60-70% of the total sulphides. It is represented by two structural varieties, hexagonal and monoclinic phases. Pyrrhotite occurs as interstitial grains, blebs, droplets, inclusions and veins in the silicates. The following textural varieties are observed: 1) blebs and droplets of monoclinic pyrrhotite containing pentlandite and chalcopyrite inclusions (Photo 1). This variety occurs mainly in the Basal and contact zones; 2) interstitial hexagonal and monoclinic pyrrhotite aggregates rimmed by pentlandite and chalcopyrite (Photo 2); 3) lamellae of monoclinic pyrrhotite in cubanite; 4) isolated pyrrhotite relicts in chalcopyrite-cubanite (Photo 3); 5) hexagonal

and monoclinic pyrrhotite in the lower portion of the polarity textured blebs; 6) pyrrhotite inclusions in plagioclase overgrowths and in augite (Photos 5 and 6).

CHALCOPYRITE(-CUBANITE) is the second most abundant sulphide. The latter always occurs as exsolution lamellae within the former, and both minerals are prominent in the Cyclic Zone. Chalcopyrite forms lenses, blebs, veins, rims and inclusions. It also appears to resorb pyrrhotite and pentlandite. The textural varieties are: 1) chalcopyrite-cubanite rims around pyrrhotite; this is the most common mode of occurrence in the mineralized zone; 2) chalcopyrite-cubanite replacement of pyrrhotite and pentlandite in the upper portion of the polarity textured blebs (Fig.2 A,B,C); 3) chalcopyrite veins, lenses and granular aggregates in monoclinic pyrrhotite of the Basal and contact zone; 4) chalcopyrite inclusions in plagioclase overgrowths, augite, and biotite; 5) interstitial and included chalcopyrite with pentlandite inclusions.

PENTLANDITE is the third most abundant sulphide. It occurs as inclusions in the above mentioned sulphides and silicates. Pentlandite inclusions may be flame shaped, granular, lenticular, bleb-like, needle-like, vein-like or irregular. They may be located in pyrrhotite, between pyrrhotite and chalcopyrite-cubanite rims, in chalcopyrite-cubanite or only in chalcopyrite. Several textural varieties are distinguished: 1) pentlandite grains, veinlets and flames in hexagonal-monoclinic pyrrhotite (Photos 2 and 4). Granular and vein pentlandite may show locally flame-like borders; 2) pentlandite grains, lenses and flames between pyrrhotite and chalcopyrite-cubanite rims; some grains may have flamelike borders; 3) remnants of incompletely replaced pentlandite in chalcopyrite-cubanite (Photo 3); 4) large pentlandite grains with hexagonal and monoclinic pyrrhotite in the lower portion of the polarity textured blebs (Photo 8); 5) pentlandite-chalcopyrite aggregates as interstitial grains or inclusions in augite that caps polarity textured blebs. This pentlandite is mostly invaded by chalcopyrite along cleavage planes ; 6) pentlandite inclusions in plagioclase overgrowths and in augite.

TROILITE occurs in minor amount associated with hexagonal pyrrhotite. It co-exists with pentlandite in olivine orthocumulates (Table 7).

VIOLARITE occurs as an alteration product of pentlandite. Violarite alteration spreads inward from the borders and cleavage planes and may replace the entire grain. Incomplete alteration results in remnants of pentlandite as islands surrounded by violarite (Table 9).

NICKELOAN PYRITE is an alteration product of pyrrhotite in the Basal and contact zones. It occurs as isolated cubic and octahedral crystals or intergrowths with the marcasite and magnetite (Table 10).

MILLERITE and BORNITE occur as isolated grains in chalcopyrite rich assemblages (Table 9, Fig.10).

NICCOLITE and MAUCHERITE form euhedral to anhedral crystals in pyrrhotite, chalcopyrite and plagioclase within the Basal and contact zones (Table 11, Fig.10).

MARCASITE is an alteration product of pyrrhotite. It is intergrown with nickeloan pyrite and magnetite (Table 10).

PYRITE and SPHALERITE are the main sulphides with chalcopyrite in the sedimentary country rocks. They form disseminations and discontinuous beds. Pyrite occurs as euhedral-subhedral crystals or anhedral aggregates. It is replaced by pyrrhotite in the contact zone of the intrusion. The textural relationships indicate that the genesis of the pyrite includes many stages of crystallization and recrystallization. It locally replaces silicates of the contact gabbros along cleavage planes or fractures, and occurs in veins with carbonates.

CHALCOPYRITE of the country rocks occurs as grains associated with other sulphides concentrated in certain of the sedimentary beds, and is also observed in fracture fillings. Sphalerite forms isolated grains associated with chalcopyrite and pyrrhotite in hornfels. It is often observed in gabbros as inclusions in chalcopyrite.

B- SULPHIDE ORE TEXTURAL VARIETIES

Sulphide ore exhibits a number of textural varieties : 1) Interstitial sulphides occupy the prismatic voids between cumulus silicates (Photo 6). Plagioclase and olivine are the two main silicates that define the outlines of sulphide grains. The latter are in general triangular and quadrangular; their size varies as a function of the size of the silicate grains which range from a fraction of a mm to 5-6 cm. Interstitial sulphide grains are commonly polyphase assemblages consisting mostly of pyrrhotite cores surrounded by chalcopyrite-cubanite rims. Apatite is a common associated mineral.

A variety of interstitial sulphides occurs in the olivine orthocumulate in which sulphides are interstitial to cumulus olivine. These grains which commonly show curved boundaries in some cases contain troilite associated with pentlandite.

2) Sulphide inclusions occur mostly in plagioclase overgrowths, augite, and biotite. When altered, Ti-magnetite in some cases contains sulphide inclusions. Plagioclase laths next to interstitial sulphides may contain sulphide inclusions in their marginal zones. The inclusions are commonly rectangular and arranged parallel to

3the (001) plane in the host plagioclase (Photo 5). These sulphides are generally chalcopyrite, pentlandite, or pyrrhotite, similar to the interstitial sulphides.

Sulphide inclusions in augite often display a eutectoid intergrowth with the host silicate (Photo 6). They are irregular or drop-like, and disseminated through the host pyroxene. Biotite in some cases partially rims sulphide grains, or completely encloses them.

3) Sulphide droplets and blebs occur in the Basal and contact rocks as well as in the sedimentary xenoliths (Photo 1). Their size ranges from 0.4 mm to 6 mm. They are often welded to each other forming aggregates of drops. Monoclinic pyrrhotite constitutes 85-90% of the droplets. Chalcopyrite forms grains, lenses, irregular crystal aggregates, and veins within droplets. In some cases chalcopyrite contains cubanite lamellae, pentlandite, or incompletely resorbed pyrrhotite grains. Pentlandite occurs as grains, granular veins and flames in pyrrhotite. Flames may start from fractures or pyrrhotite-chalcopyrite boundaries. Some pentlandite veins exhibit flame-like borders. Niccolite and maucherite are often observed as euhedral to subhedral grains in Basal zone pyrrhotite.

4) Myrmekitic sulphides are intergrown with orthopyroxene at the edge of olivine (Photo 7). The worm-like sulphide may be chalcopyrite, pyrrhotite or pentlandite. This texture occurs when olivine reacted with intercumulus plagioclase to form orthopyroxene, biotite and ilmenite.

5) Sulphide veins appear to comprise two generations. The first is primary and contemporaneous with the segregation of the sulphide immiscible liquid. These veins crosscut all host silicates and connect the interstitial sulphide grains to each other. Their mineralogy is the same as the connected grains, namely chalcopyrite, pyrrhotite and pentlandite. The second type of sulphide veins is secondary, occurs only in serpentinized olivine, and commonly comprises pyrrhotite together with magnetite.

6) Mineral assemblage polarity (MAP) textured blebs are recognized in the Mixed and Cyclic zones. A similar sulphide texture is described by Eckstrand (1980) in a komatiitic nickel deposit in the Timmins area, Ontario. These blebs in the Cyclic Zone exhibit a number of systematic textural characteristics (Fig. 2 A, B and C).

a) The lower part of each sulphide bleb is interstitial to surrounding silicates (generally plagioclase), while the upper part of the bleb is intergrown with augite, which forms a capping over the bleb.

b) The adjoining plagioclase laths contain numerous sulphide inclusions in their marginal zones while the capping augite includes eutectoid-like sulphide grains.

c) The blebs consist of two zones. An upper zone is composed mainly of chalcopyrite-cubanite which contains numerous islands of partially resorbed pyrrhotite and pentlandite. In some instances, apatite forms large crystals scattered in the upper zone (Fig. 2B). The lower zone consists mainly of pyrrhotite which is rimmed by large pentlandite grains up to 1 mm in size. Depending upon the section, the chalcopyrite-rich upper zone or the pyrrhotite-rich lower one may dominate in a single bleb.

d) Chalcopyrite with high-Ni pentlandite inclusions is found in capping augite or in single interstitial grains.

e) The pyrrhotite of the lower portion consists of hexagonal and/or monoclinic phases, or more rarely troilite. Mackinawite is commonly observed in pentlandite and chalcopyrite.

f) In cases where chrome spinel occurs together with these MAP textured sulphides, it forms large irregular crystals in the plagioclase overgrowth zone and augite. These spinels are the largest and commonly contain ilmenite exsolution lamellae.

COMPOSITIONAL VARIATIONS OF THE MAIN SULPHIDES

1- PENTLANDITE exhibits a wide range of Fe, Ni and Co contents which appear to be related to the sulphide assemblage and to stratigraphic height within the intrusion.

A-Nickel variations in pentlandite.

Nickel in pentlandite correlates negatively with Fe and Co contents, and ranges from 25.64 to 38.69 wt%, while the corresponding Fe ranges from 40.18 wt% to 27.58 wt % (Tables 3 to 6).

Ni content of pentlandite in natural and artificial systems has been demonstrated to be related to the compositions of the co-existing sulphides (Graterol and Naldrett 1971; Harris and Nickel, 1972; Misra and Fleet, 1973). The following four sulphide assemblages in the GLN deposit control Ni content of pentlandite: 1) troilite-pentlandite; 2) hexagonal pyrrhotite-pentlandite; 3) monoclinic pyrrhotite-pentlandite; 4) chalcopyrite-pentlandite. Troilite-pentlandite is observed in olivine orthocumulates of the Cyclic zone. Hexagonal pyrrhotite-pentlandite occurs in both the Cyclic and the Cu-Ni mineralized zones. Monoclinic pyrrhotite-pentlandite is dominant in the basal and contact zones. Chalcopyrite-pentlandite is mainly observed in the Cyclic zone, but is found locally in the Lower Unlayered Zone. Ni content variations are plotted in the Fe-Ni-S diagram of Fig. 3. Pentlandite associated with troilite is poorest in Ni, and ranges from 25.64 to 29.61 wt% (Table 6). That associated with hexagonal pyrrhotite contains 30.41 to 34.35 wt% Ni. Pentlandite co-existing with monoclinic pyrrhotite has higher Ni content, ranging from 31.20 wt% to 35.87 wt% . Pentlandite inclusions within chalcopyrite have the highest Ni content, lying between 35.73 wt% and 38.69 wt% (Table 5). The latter values correspond to those in pyrite-pentlandite-pyrrhotite assemblages or in smythite-pentlandite-pyrrhotite assemblages (Harris and Nickel 1972), although smythite and primary pyrite have not been observed in the Crystal Lake intrusion. Nickeliferous pyrite and pyrite of the basal and contact zones are secondary in origin.

B-Cobalt variations in pentlandite.

Co content of pentlandite tends to reflect two factors: 1) stratigraphic position within the intrusion, and 2) the presence of the sedimentary xenoliths. Variations in Co and Ni content in pentlandite tend to be antipathetic, and they correlate negatively with each other. This is shown in Fig. 4 and 5, which also display the high Co content of pentlandites associated with monoclinic pyrrhotites.

The xenoliths are considered to be of supracrustal origin, and contain pentlandite having high Co and low Ni contents. The Cyclic Zone pentlandite is poorer in Co, generally less than 1 wt%, but Co content increases with depth in the intrusion to a maximum of about 7.4 wt% in the contact zone and in xenoliths. Fig. 6.

In the binary diagram of Fig. 6, Co contents are plotted versus metal/sulphur ratios of pentlandite in different zones. This diagram together with those of the Figures 4 and 5 lead to the following conclusions: 1) Cyclic Zone pentlandite is the lowest in Co content; 2) Co content increases with depth in the intrusion. Pentlandite in the Basal and contact zones as well as in xenoliths is the richest in Co; 3) Basal and contact zone pentlandite is associated with monoclinic pyrrhotite, but its Ni content is slightly lower than normal, presumably because of the high Co content. 4) In spite of the general Co enrichment with depth, in detail Co content is erratic.

2- PYRRHOTITE exhibits the normal compositional variations depending upon the structural phase. Hexagonal pyrrhotites are richer in iron, having an Fe content ranging from 60.29 to 61.97 wt% (Table 1), while monoclinic pyrrhotite has 58.17 to 59.74 wt% Fe (Table 2). Fig. 7.

The Ni and Co content of pyrrhotite is low, generally below 0.8 wt% . Monoclinic pyrrhotite is richer in Ni and Co than hexagonal pyrrhotite (Fig. 8 and 9), though this may simply reflect the high Ni and Co content of pentlandite co-existing with monoclinic pyrrhotite.

3- CHALCOPYRITE and CUBANITE do not exhibit any significant compositional variations. Microprobe analyses of these minerals from different zones of the intrusion are given in Table 8.

COMPARISON WITH THE DULUTH COMPLEX DEPOSITS

The Crystal Lake intrusion is genetically related to the Duluth Complex (Minnesota) with which it shares numerous characteristics. Both intrusions were emplaced about 1,1 Ga ago during the formation of the Midcontinent Rift (Goldich et al., 1961; Chase and Gilmer, 1973). The Cu-Ni mineralization in the Duluth Complex lie within a few hundred metres of the basal contact (Bonnichsen, 1972b; Foose and Weiblen, 1986). The Animikian Virginia Formation, Biwabik Iron Formation and Archean Giants Range Granites constitute the basement to the Duluth complex. The Rove Formation which hosts the Crystal Lake intrusion is equivalent of the Virginia Formation. Drill holes in the eastern part of the intrusion intersected granitic rocks lying under the Crystal Lake gabbros. The basal zones of both

intrusions contain abundant hornfels xenoliths (Bonnichsen, 1972a; Phinney, 1972; Cogulu, 1988a).

The mineralogy of the sulphide deposits of the Duluth Complex is similar to that of the Great Lakes Nickel deposit. Pyrrhotite is generally dominant with less abundant chalcopyrite and minor pentlandite (Bonnichsen, 1972b; Weiblen and Morey, 1976; Tyson and Chang, 1984). Similar sulphide textures were also described in the Duluth deposits (Weiblen and Morey, 1976; Tyson and Chang, 1984; Pasteris, 1984). However the MAP-textured blebs, and sulphide droplets in hornfels observed in the Crystal Lake intrusion, have not been reported in the Duluth Complex.

Systematic variations of the Ni and Co contents of pentlandite in relation to coexisting sulphides and stratigraphic depth have not been documented in the Duluth deposits. Pasteris (1984) described assemblages of troilite with low-Ni pentlandite (29.88 wt% Ni), and high-Ni pentlandite (42.72 wt% Ni) with chalcopyrite. As to the Co content of the pentlandites, Foose and Weiblen (1986) gave an average of 1.84 wt%. Ripley and Alawi(1986) recorded a Co range from 0.6 to 5.0 wt% in the Babbitt deposit.

DISCUSSION AND INTERPRETATION

The preceding descriptions and data provide strong evidence for cobalt contamination of the intrusion. The high Co content of pentlandite in hornfels xenoliths, and the increase in Co with depth in the intrusion are consistent with the assimilation of country rocks by gabbroic magma. The Cyclic Zone apparently is unaffected by this contamination as suggested by the low-Co content of its pentlandite.

Sulphur isotope and Se/S analytical data given by Eckstrand and Cogulu (1986) provide convincing evidence of sedimentary origin of the sulphur that was involved in the genesis of sulphide mineralization in the Crystal Lake intrusion. In addition, silica and potash are enriched in the gabbro next to sedimentary xenoliths and contact zones.

The presence of heterogeneous gabbros with anastomosing felsic veins in the Basal Zone may indicate another contamination mechanism, the mixing of magma with partial melting products of the country rocks (Cogulu, 1988a). The introduction of silica by partial melts could initiate sulphide saturation. As suggested by Irvine (1977) blending of a basic magma with a silica rich melt could produce segregation of immiscible sulphide liquid. But high sulphide concentrations of the GLN deposit are not exclusive to areas of partial melt contamination. This may indicate that silica introduction has no direct bearing on sulphide saturation.

The textural and chemical features that have been described suggest two possible mechanisms of contamination that may have led to the generation of the Cu-Ni mineralization of the GLN deposit: 1) devolatilization of the country rocks, and 2) assimilation of sedimentary xenoliths. Textural relationships demonstrate that the separation of sulphides is contemporaneous with crystallization of plagioclase overgrowth zones and augite. In other words, sulphides are all intercumulus. Cl-apatite prisms and euhedral biotites are often associated with chalcopyrite rich assemblages and MAP- textured blebs. These indicate that volatiles were present along with the immiscible sulphide melt. The MAP-textured blebs consist of a pyrrhotite rich lower portion overlain by a chalcopyrite rich upper portion and associated apatite and biotite. These may be interpreted to represent fractional crystallization of sulphide liquid to produce, first, gravitationally segregated mss, and then iss together with volatile-bearing gangue minerals. According to experimental work in the system Cu-Fe-Ni-S, a sulphide liquid crystallizing mss can be progressively enriched in copper by fractional crystallization (Craig and Kullerud, 1969).

Sulphide disseminations in the Great Lakes Nickel deposit are generally concentrated in the axial or keel zone of the intrusion. This may indicate that sulphide melt migrated toward the keel zone in the elongate basin. This migration may have occurred in small scale through the silicate framework. Polygonal sulphides showing linear boundaries with plagioclase laths which do not contain included grains may represent migrated immiscible liquid.

In natural and synthetic Fe-Ni-S systems, the composition of pentlandite is related to the mineralogy of the coexisting sulphides (Graterol and Naldrett, 1971; Harris and Nickel, 1972). In general, pentlandite with high Ni content occurs in assemblages containing pyrite, smythite or millerite. None of these sulphides is found as primary minerals coexisting with pentlandite in the GLN deposit. The Ni content of pentlandite inclusions in chalcopyrite are not enough high to be associated with millerite, although this latter mineral does occur in the deposit as an alteration product (Table 7, Fig.10). All these considerations may suggest that the high Ni content of the pentlandite in pentlandite-chalcopyrite assemblages could be due to reequilibration during the late stages of the mineralization. As described above, chalcopyrite commonly appears to resorb the earlier pyrrhotite and pentlandite. Cubanite lamellae related to this resorbition consumed FeS of the resorbed pyrrhotites. Nickel of the resorbition would be diffused into pentlandites during reequilibration. The lamellae-like chalcopyrite which cross-cuts the high-Ni pentlandites would be due to the differences in contraction indices of these minerals.

Chrome spinels occurring with MAP-textured blebs are mostly large crystals. They are also enriched in Fe³⁺ and Ti. This is due to the reaction with the trapped liquid before the separation of the sulphide immiscible melt (Cogulu, 1990b).

The metal/sulphur ratio of the pentlandite is about 0.6 in atomic proportions. As a result of this, when Co content increases Ni content decreases. This negative correlation is illustrated in Fig.4. This relationship should be taken into consideration when determining economic potential of the deposit.

CONCLUSIONS

There are two distinct populations of sulphide in the Crystal Lake intrusion. The major sulphides of both populations are pyrrhotite, chalcopyrite, cubanite, and pentlandite. The older population occurs in the Basal and Lower Unlayered Zones, and forms massive and disseminated ore. It is mainly composed of pyrrhotite, of which the monoclinic phase is dominant in the Basal and contact zones. Hexagonal pyrrhotite which locally may contain minor troilite occurs in the Lower Unlayered Zone.

The second sulphide population forms low grade dissemination in the Cyclic Zone. Chalcopyrite and cubanite are dominant, and troilite may locally co-exist with pentlandite. The magma that produced the Cyclic units was poorer in sulphur, and massive sulphide is not observed, though MAP-textured blebs are common. The fractionation of these blebs into pyrrhotite bottoms and chalcopyrite tops appears to have been systematically accompanied by enrichment of volatiles that produced apatite and biotite.

Pentlandite exhibits systematic compositional variations in Co and Ni content. Co content of pentlandite increases with depth in the intrusion and attains about 7 wt% in the basal contact zones. This enrichment is probably the result of assimilation of country rocks that contained Co-bearing sulphides. The cyclic zone pentlandite is poor in Co (less than 1 wt%).

Ni content of pentlandite is related to co-existing sulphides. The lowest Ni content (about 25 wt% to 29 wt%) occurs in pentlandite associated with troilite. Progressively higher Ni contents occur in pentlandite associated respectively with monoclinic pyrrhotite, hexagonal pyrrhotite, and chalcopyrite. In the last of these assemblages, pentlandite contains about 36 to 39 wt% Ni.

Assimilation and devolatilisation of the contact sedimentary rocks associated with the emplacement of the intrusion was the principal source of sulphur in the generation of Cu-Ni sulphide mineralization. Contamination by mixing with products of partial melting of the contact rocks caused increase in the silica content of the magma, but this apparently had no significant influence in producing sulphide saturation. Segregation of an immiscible sulphide melt gave first an Fe-Ni-rich mss and later a Cu-rich iss by fractional crystallization.

ACKNOWLEDGMENTS

The author thanks especially O.R. Eckstrand at the Geological Survey of Canada for valuable comments during the research. J.M. Duke, R.F.J. Scoates and D.C. Harris are also thanked for their excellent suggestions. Help with mineral determinations by D.C. Harris, and assistance with microprobe analyses by G.J. Pringle, M. Bonardi, and G. Lecheminant are gratefully acknowledged. R.M. Laramée is thanked for assistance with computer aspects of printing. Boliden Canada Ltd. and J.P. McGoran of Fleck Resources kindly provided access to the property and drill core.

This study was financially supported by grant A0590 of the Natural Sciences and Engineering Research Council of Canada, and by the Geological Survey of Canada through contract under the Canada-Ontario Mineral Development Agreement.

REFERENCES

- Bonnichsen, B., 1972, Sulphide minerals in the Duluth Complex; in *Geology of Minnesota: a Centennial Volume*, P.K. Sims and G.B. Morey, eds., Minnesota Geological Survey, Spec. Vol., p.388-393.
- Chase, C.G. and Gilmer, T.H., 1973, Precambrian plate tectonics: the midcontinent gravity high. *Earth Planetetary Science Letters*, v.21, p.70-78.
- Cogulu, E.H., 1985, Platinum group elements and chromian spinel variations in the Crystal Lake gabbros, Thunder Bay, Ontario. Fourth Int. Platinum Symp. Abstr. *Can. Mineral.* v.23, p.299-300.
- Cogulu, E.H., 1990, Mineralogical and petrological studies of the Crystal Lake intrusion, Thunder Bay, Ontario; Open File. Geological Survey of Canada.
- Cogulu, E.H. 1993, Factors controlling postcumulus compositional changes of chrome-spinels in the Crystal Lake intrusion, Thunder Bay, Ontario. Open File. Geological Survey of Canada.
- Craig, J.R. and Kullerud, G., 1969, Phase relations in the Cu-Fe-Ni-S system and their application to magmatic ore deposits; in *Magmatic Ore Deposits*, H.D.B. Wilson, ed., *Economic Geology Monograph* 4, p.344-358.
- Craig, J.R., 1973, Pyrite-pentlandite assemblages and other low temperature relations in the Fe-Ni-S systems, *American Journal Science*, v.273-A, p.496-510.
- Davidson, J.M. Jr., 1982, Geological evidence relating to interpretation of the Lake Superior Basin structure, *Geological Society America Memoir* 156, p.5-14.
- Eckstrand, O.R., 1980, Mineral assemblage polarity in magmatic sulphide blebs in a komatiitic nickel deposit; in *Geological Survey Canada Paper* 80-1A, p.385-389.
- Eckstrand, O.R. and Cogulu, E.H., 1986, Se/S evidence relating to genesis of sulphides in the Crystal Lake Gabbro, Thunder Bay, Ontario; *Geological Association Canada/Mineralogical Association Canada Annual Meeting, Program with Abstracts*, v.11, p.66.
- Faure, G., Chaudhuri, S. and Fenton, M.D., 1969, Ages of the Duluth Gabbro Complex and of the Endion Sill, Duluth, Minnesota; *Journal Geophysical Research*, v.74, p.720-725.

- Franklin, J.M., Shegelski, R.J., McIlwayne, W.H., Mitchell, R.H. and Platt, R.G., 1982, Proterozoic Geology of the Northern Lake Superior Area; Geological Association Canada/Mineralogical Association Annual Meeting, Field Trip 4 Guidebook.
- Geul, J.J.C., 1970, Geology of Devon and Pardee Townships and the Stuart Location; Ontario Department Mines, Geological Report 87, p.52.
- Goldich, S.S., Nier, A.O., Baadsgaard, H., Hoffman, J.H. and Kraeger, H.W., 1961, The Precambrian geology and geochronology of Minnesota; Minnesota Geological Survey, Bulletin 43, 193p.
- Graterol, M. and Naldrett, A.J., 1971, Mineralogy of the Marbridge No.3 and No.4 nickel-iron sulphide deposits, with some comments on low temperature equilibration in the Fe-Ni-S system; *Economic Geology* v.66, p.879-900.
- Harris, D.C. and Nickel, E.H., 1972, Pentlandite compositions and associations in some mineral deposits; *Canadian Mineralogist*, v.11, p.861-878.
- Irvine, T.N., 1977, Origin of chromitite layers in the Muskox intrusion and other stratiform intrusions: a new interpretation; *Geology*, v.5, p.273-277.
- Mainwaring, P.R., 1968, The sulphide assemblage of the Great Lakes Nickel Intrusion; B.Sc. thesis, University Western Ontario, London, Ontario.
- Mainwaring, P.R. and Naldrett, A.J., 1977, Country rock assimilation and the genesis of Cu-Ni sulfides in the Waterhen intrusion, Duluth Complex, Minnesota, *Economic Geology*, v. 72, p.1269-1284.
- Misra, K.C. and Fleet, M.E., 1973, The chemical composition of synthetic and natural pentlandite assemblages; *Economic Geology*, v.68, p.518-539.
- Pasteris, J.D., 1984, Further interpretation of the Cu-Fe-Ni sulfide mineralization in the Duluth Complex, Northeastern Minnesota, *Canadian Mineralogist* v.22, p.39-53.
- Phinney, W.C., 1972, Northwestern part of Duluth Complex; in *Geology of Minnesota: a Centennial Volume*, P.K.Sims and G.B. Morey, eds., Minnesota Geological Survey Special Volume, p.335-360.
- Ripley, E.M., 1986, Application of stable Isotopic studies to problems of magmatic sulfide ore genesis with special reference to the Duluth Complex, Minnesota, in *Geology and Metallogeny of Copper Deposits*; G.H.Friedrich et al., eds., Springer Verlag, p.25-42.

Ripley, E.M. and Alawi, J.A., 1986, Sulfide mineralogy and chemical evolution of the Babbitt Cu-Ni deposit, Duluth Complex, Minnesota; *Canadian Mineralogist*, v.24, p.347-368.

Tyson, R.M., and Chang, L.L.Y., 1984, The petrology and sulfide mineralization of the Partridge River troctolite, Duluth Complex, Minnesota. *Canadian Mineralogist*, v.22, p.23-38.

Weiblen, P.W. and Morey, G.B., 1976, Textural and compositional characteristics of sulfide ores from the basal contact zone of the South Kawishiwi intrusion, Duluth Complex, Northeastern Minnesota, *Proceedings 37th Annual Mining Symposium*, Minnesota Geological Survey, Reprint Series 32.

FIGURES

- Fig. 1. Geological map of the Crystal Lake area (modified after Geul, 1970). Star indicates location of surface samples; full circles, drill holes.
- Fig. 2A. Oriented vertical section of a sulphide bleb showing mineral assemblage polarity (MAP). The pyrrhotite-pentlandite-rich lower zone is overlain by the chalcopyrite-cubanite-apatite-rich upper zone. AUG = capping augite, BIO = biotite, APT = apatite, CP-CB = chalcopyrite-cubanite, PO = pyrrhotite, PE = pentlandite, CR = chrome spinel; the arrow points stratigraphically upward. Sample 292/1/2, Cycle 2 of the Cyclic Zone.
- Fig. 2B. Oriented vertical section of MAP-textured sulphide bleb. Sample 140C, Cycle 1. Symbols are the same as in Fig. 2A.
- Fig. 2C. Oriented vertical section of MAP-textured sulphide bleb. Sample 294/1 Cycle 2. Symbols are the same as in Fig. 2A.
- Fig. 3. Nickel contents of pentlandite (atomic proportions) associated with different iron sulphides. Crosses = pentlandites associated with troilite; filled rectangles = pentlandites associated with hexagonal pyrrhotite; X's = pentlandites associated with monoclinic pyrrhotite; open circles = pentlandite inclusions within chalcopyrite.
- Fig. 4. Cobalt vs. nickel contents (weight percent) of pentlandite. Open triangles = pentlandites associated with hexagonal pyrrhotites; crosses = pentlandites associated with monoclinic pyrrhotites; open circles = pentlandite inclusions within chalcopyrite; X's = pentlandites associated with troilite.
- Fig. 5. Cobalt content of pentlandite (atomic proportions) associated with different iron sulphides. Symbols are the same as in Fig. 4.
- Fig. 6. Cobalt content (weight percent) vs. metal/sulphur ratio of pentlandite in relation to its petrological environment in the intrusion. Crosses = Cyclic Zone; open circles = Lower or mineralized zone; X's = Contact Zone; filled rectangles = xenoliths. A = pentlandite inclusions within chalcopyrite; B = pentlandites associated with hexagonal pyrrhotites; C = pentlandites associated with monoclinic pyrrhotites.
- Fig. 7. Iron vs. sulphur content (atomic percent) of pyrrhotite. Open triangles = hexagonal pyrrhotites; crosses = monoclinic pyrrhotites.
- Fig. 8. Cobalt vs. nickel content (weight percent) of pyrrhotite. Open triangles = hexagonal pyrrhotites; crosses = monoclinic pyrrhotites.

Fig. 9. Cobalt vs. sulphur (atomic percent) of pyrrhotites. Symbols are the same as in Fig.8.

Fig. 10. Compositions (atomic percent) of accessory sulphides as plotted in Fe-Ni-S and Fe-Ni-As diagrams.

PHOTOGRAPHS

Photo 1 Droplets of sulphides in hornfels. Chalcopyrite and pentlandite grains are irregularly disseminated. Magnification $\times 25$. Sample 201/505, Contact Zone.

Photo 2 Interstitial sulphides composed of pyrrhotite, chalcopyrite and pentlandite. Pyrrhotite is rimmed by pentlandite and chalcopyrite. Apatite forms euhedral prismatic crystals. Magnification $\times 33$.
Sample DH18-160. Mineralized zone.

Photo 3 Pyrrhotite and pentlandite relicts in chalcopyrite which contains cubanite lamellae. Magnification $\times 25$.
Sample 130A. Cyclic zone.

Photo 4 Pentlandite flames and grains which rim interstitial pyrrhotite. Magnification $\times 25$.
Sample 200/462. Mineralized zone.

Photo 5 Interstitial and included sulphides. Pyrrhotite is rimmed by chalcopyrite-cubanite and pentlandite. Included sulphide grains within plagioclase laths are chalcopyrite, pyrrhotite and pentlandite. They lie along the 001 planes in plagioclase. Magnification $\times 25$.
Sample 212/400. Mineralized zone.

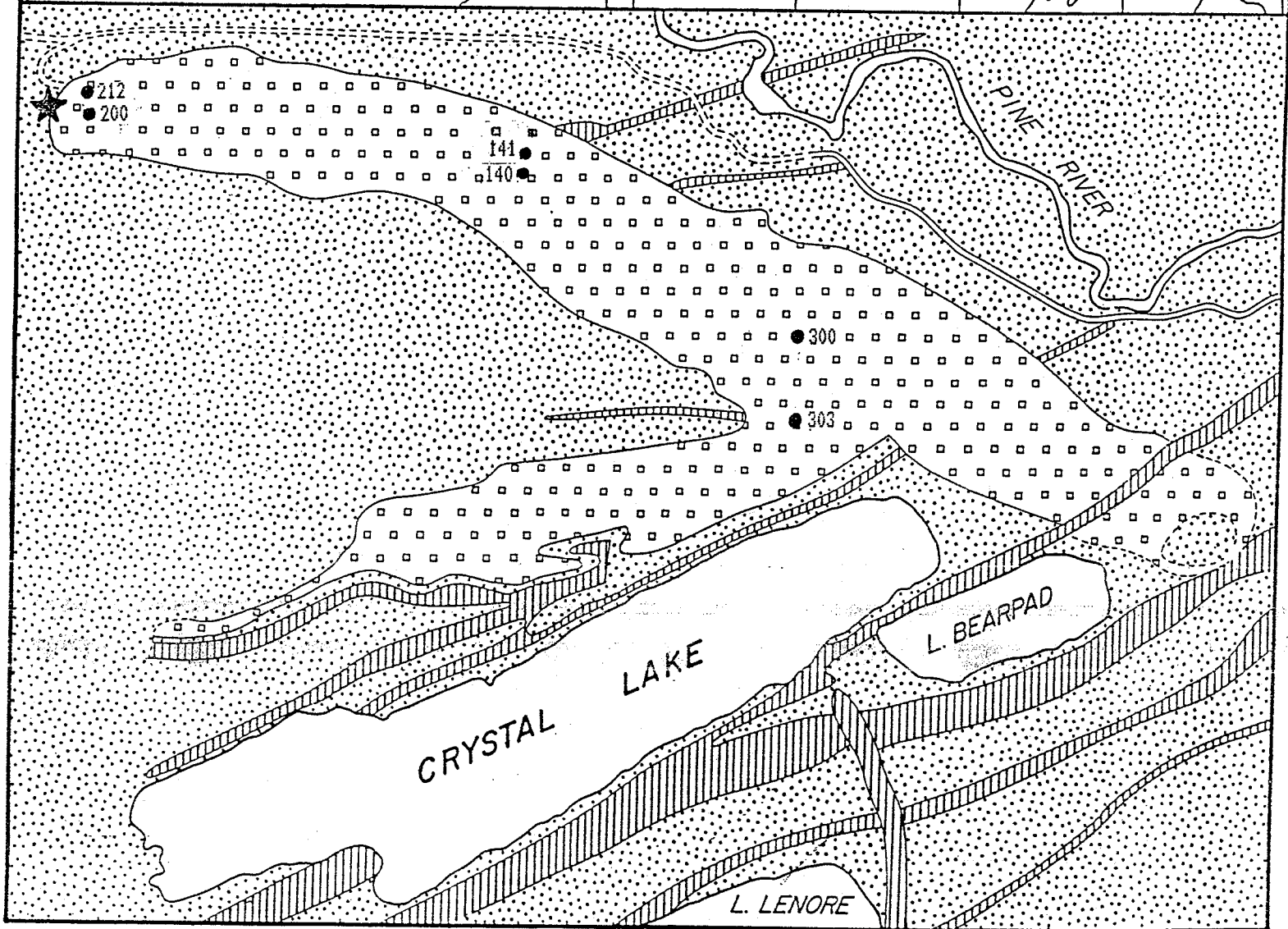
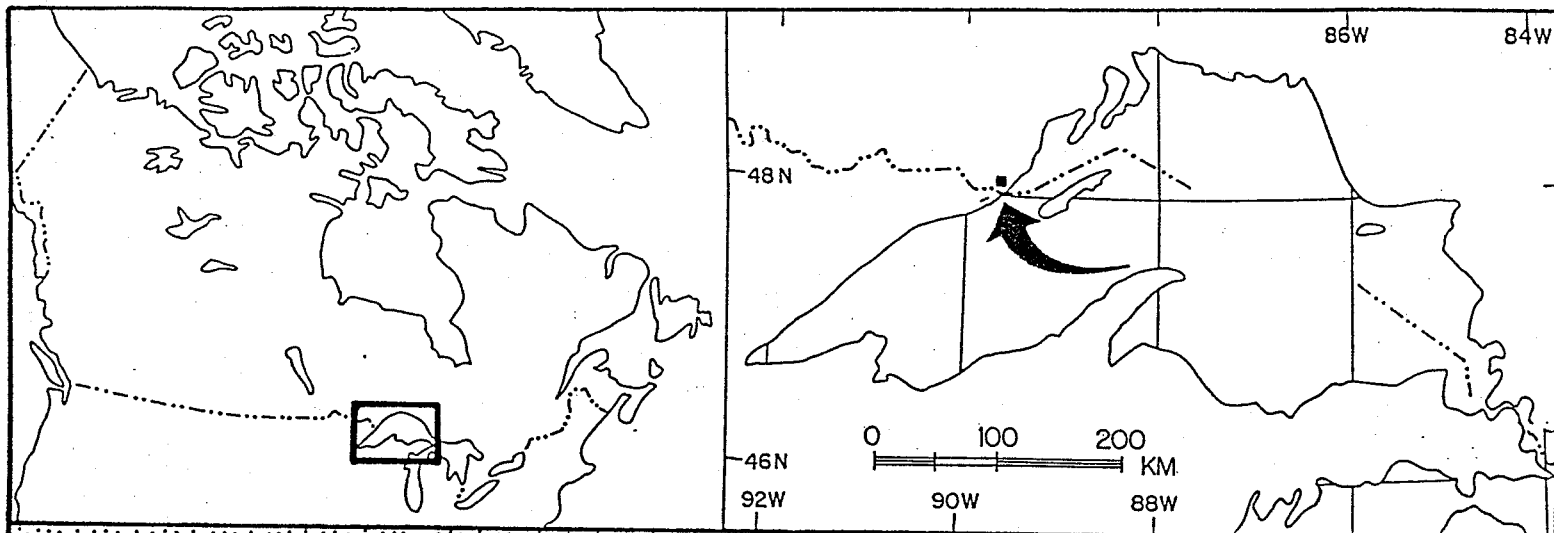
Photo 6 Included and interstitial sulphides. Included sulphides exhibit an eutectoid relationship with the host augite. In the left portion of the photo, polyhedral sulphide grains are interstitial to plagioclases.
Sample 160/2. Magnification $\times 8$. Cyclic Zone.

Photo 7 Sulphide-silicate myrmekitic intergrowths. Chalcopyrite and pyrrhotite exhibit a myrmekitic intergrowth with orthopyroxene. (APT: apatite, PLG: plagioclase, olv: olivine). Magnification $\times 25$.
Sample DH18/80. Mineralized zone.

Photo 8 Large pentlandite grains and minor chalcopyrite rim the lower pyrrhotite of a MAP-textured bleb. Included sulphide grains lie along 001 planes of the plagioclase.
Magnification $\times 25$. Sample 130/A. Cyclic Zone.

TABLES

- | | |
|----------|--|
| Table 1 | Electron microprobe analyses of hexagonal pyrrhotite. |
| Table 2 | Electron microprobe analyses of monoclinic pyrrhotite. |
| Table 3 | Electron microprobe analyses of pentlandite associated with monoclinic pyrrhotite. |
| Table 4 | Electron microprobe analyses of pentlandite associated with hexagonal pyrrhotite. |
| Table 5 | Electron microprobe analyses of pentlandite associated with chalcopyrite. |
| Table 6 | Electron microprobe analyses of pentlandite associated with troilite. |
| Table 7 | Electron microprobe analyses of troilite. |
| Table 8 | Electron microprobe analyses of chalcopyrite and cubanite. |
| Table 9 | Electron microprobe analyses of violarite, mackinawite, bornite and millerite. |
| Table 10 | Electron microprobe analyses of nickeloan pyrite, pyrite and nickeloan marcasite. |
| Table 11 | Electron microprobe analyses of niccolite and maucherite. |





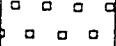
-  SEDIMENTARY ROCKS (ROVE FORMATION) AND GLACIAL DEPOSITS
-  PIGEON RIVER DIABASE DYKES
-  CRYSTAL LAKE GABBROIC INTRUSION



Fig. 1

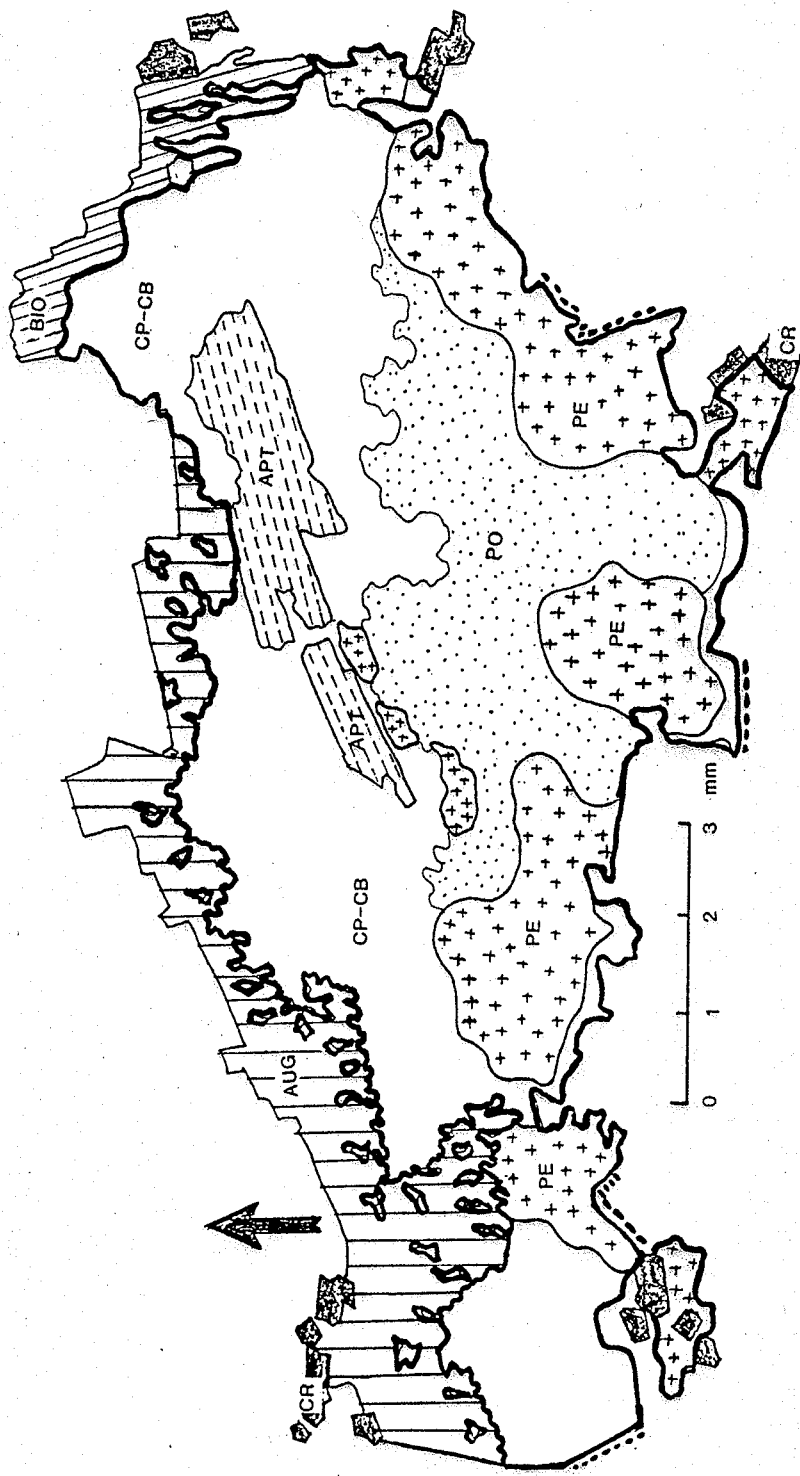


Fig.2 A

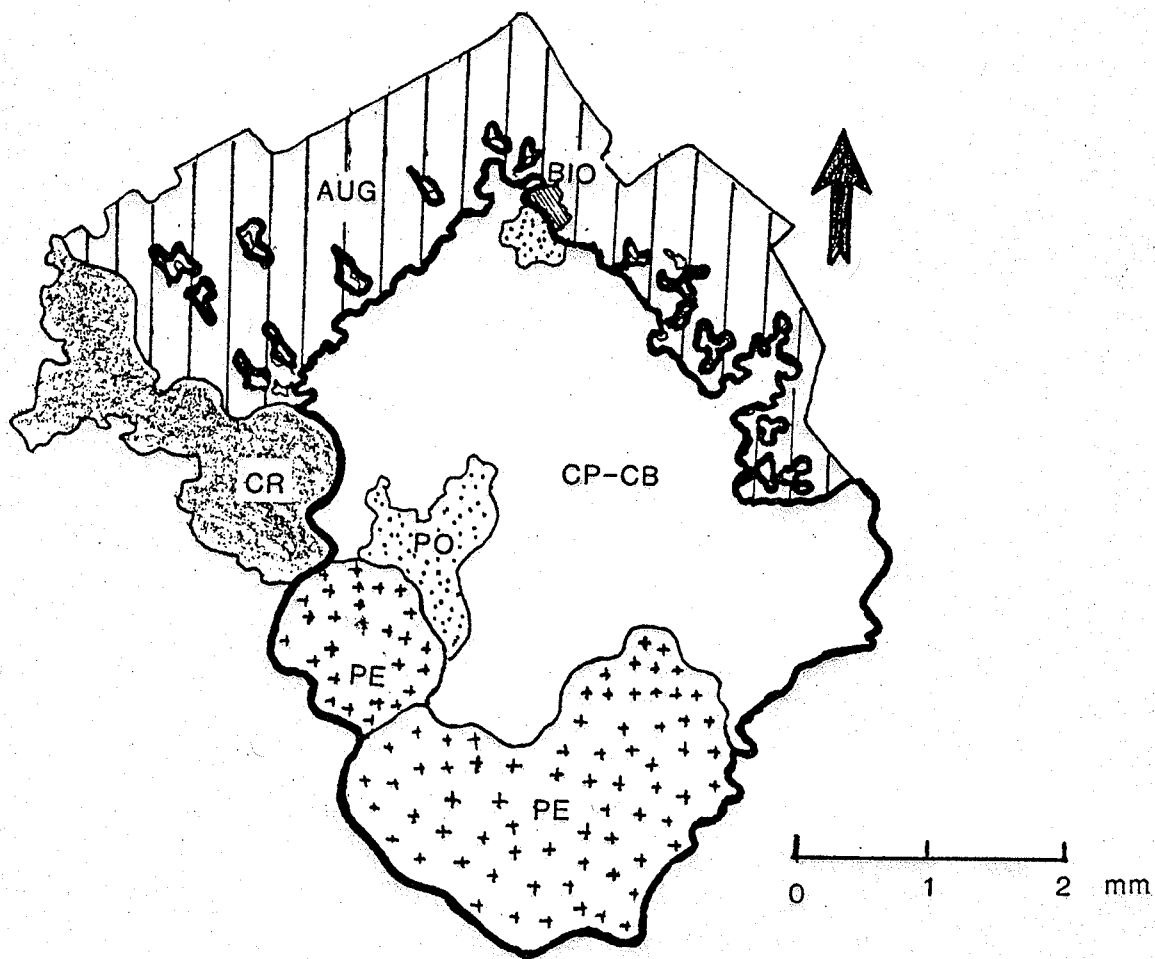


Fig.2 B

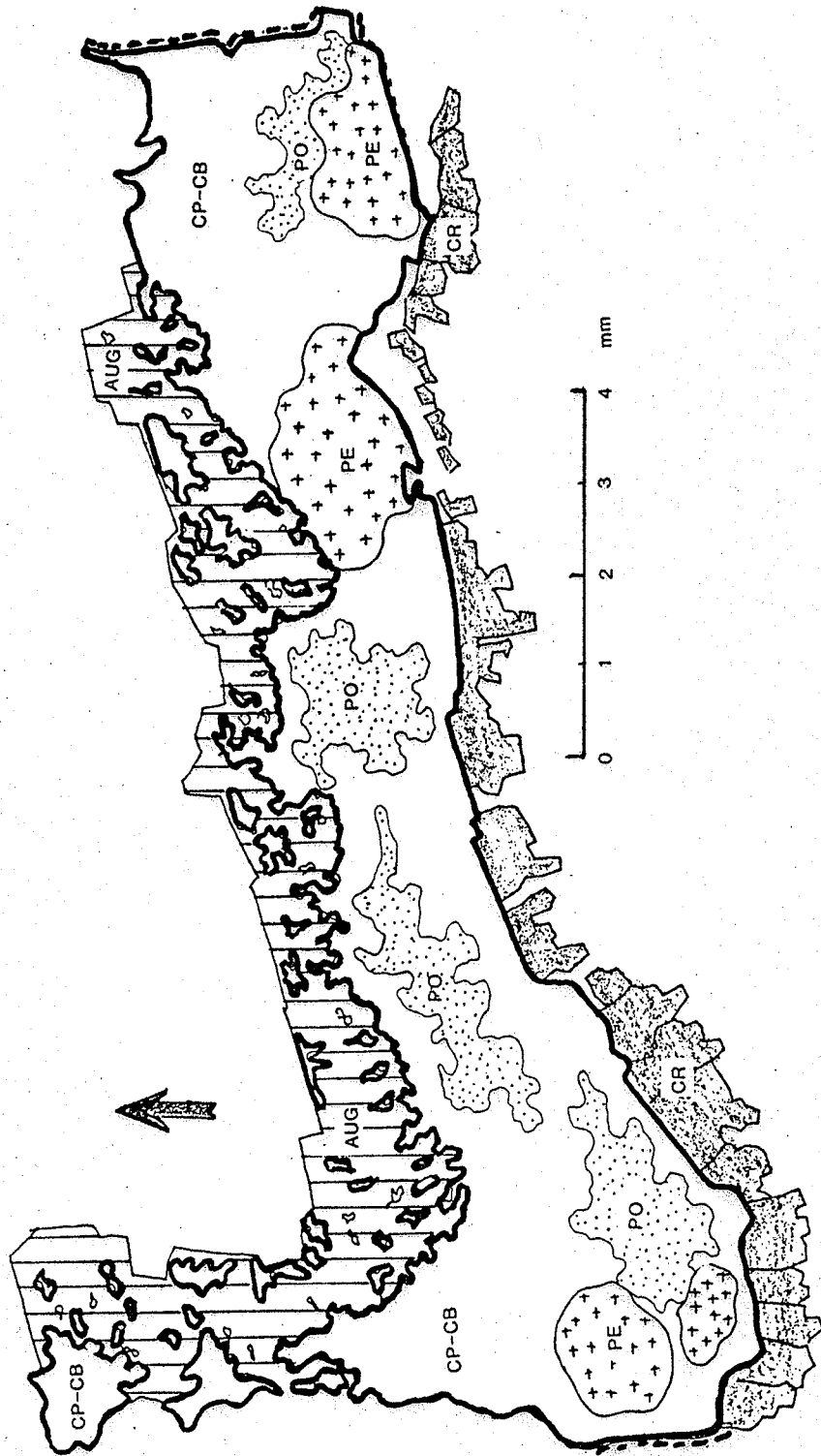


Fig. 2 C

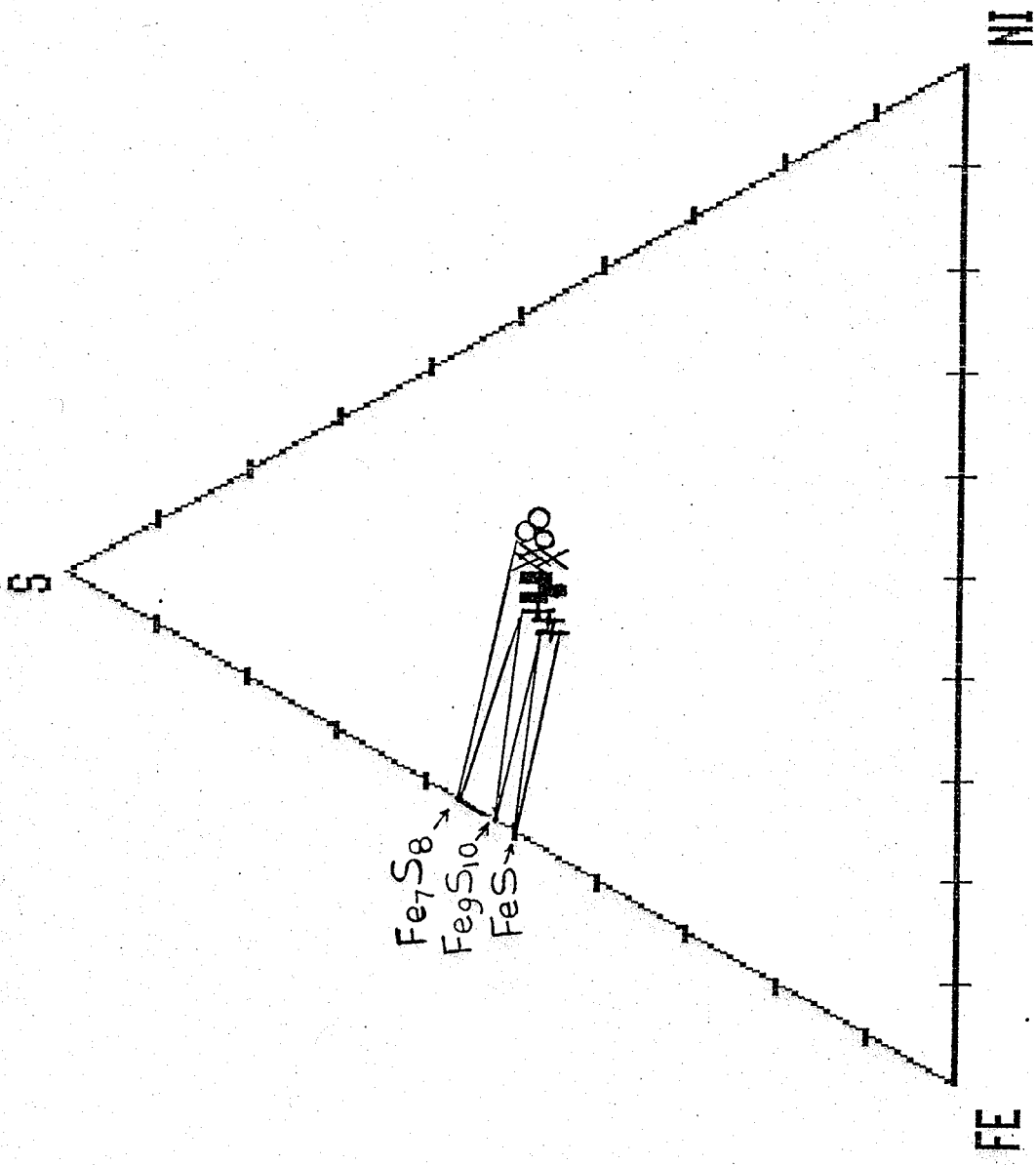


Fig. 3

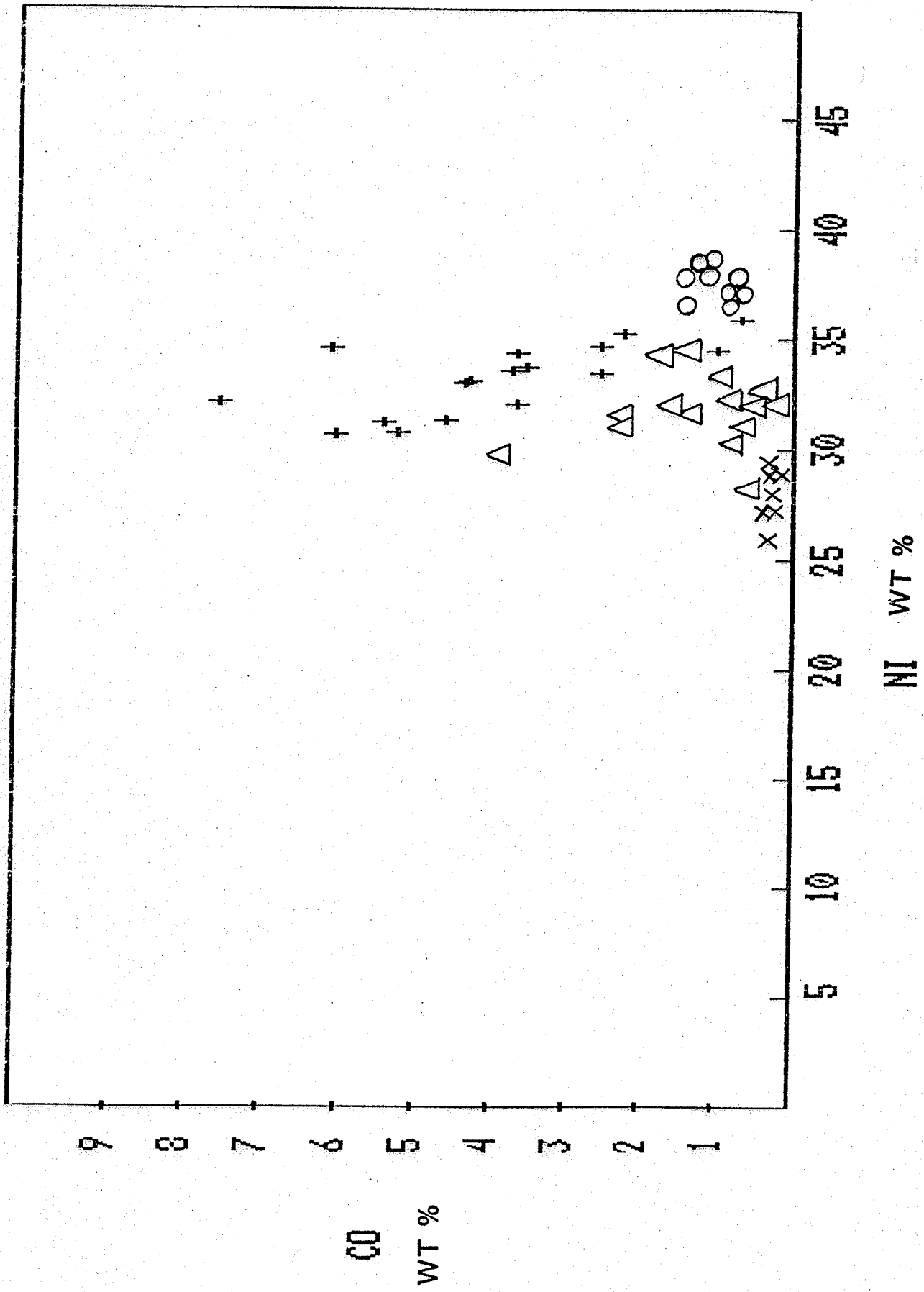


Fig. 4

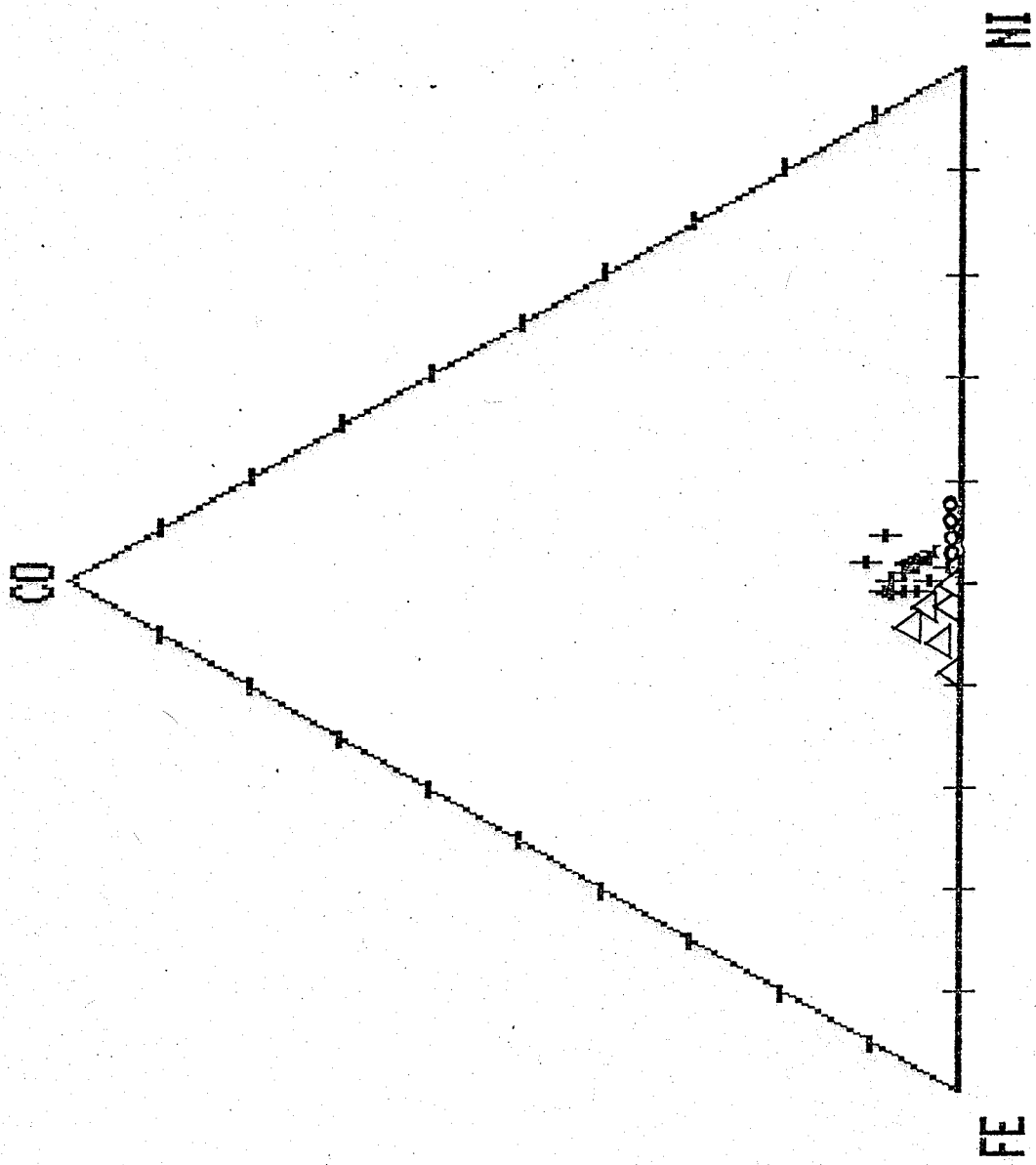


Fig. 5

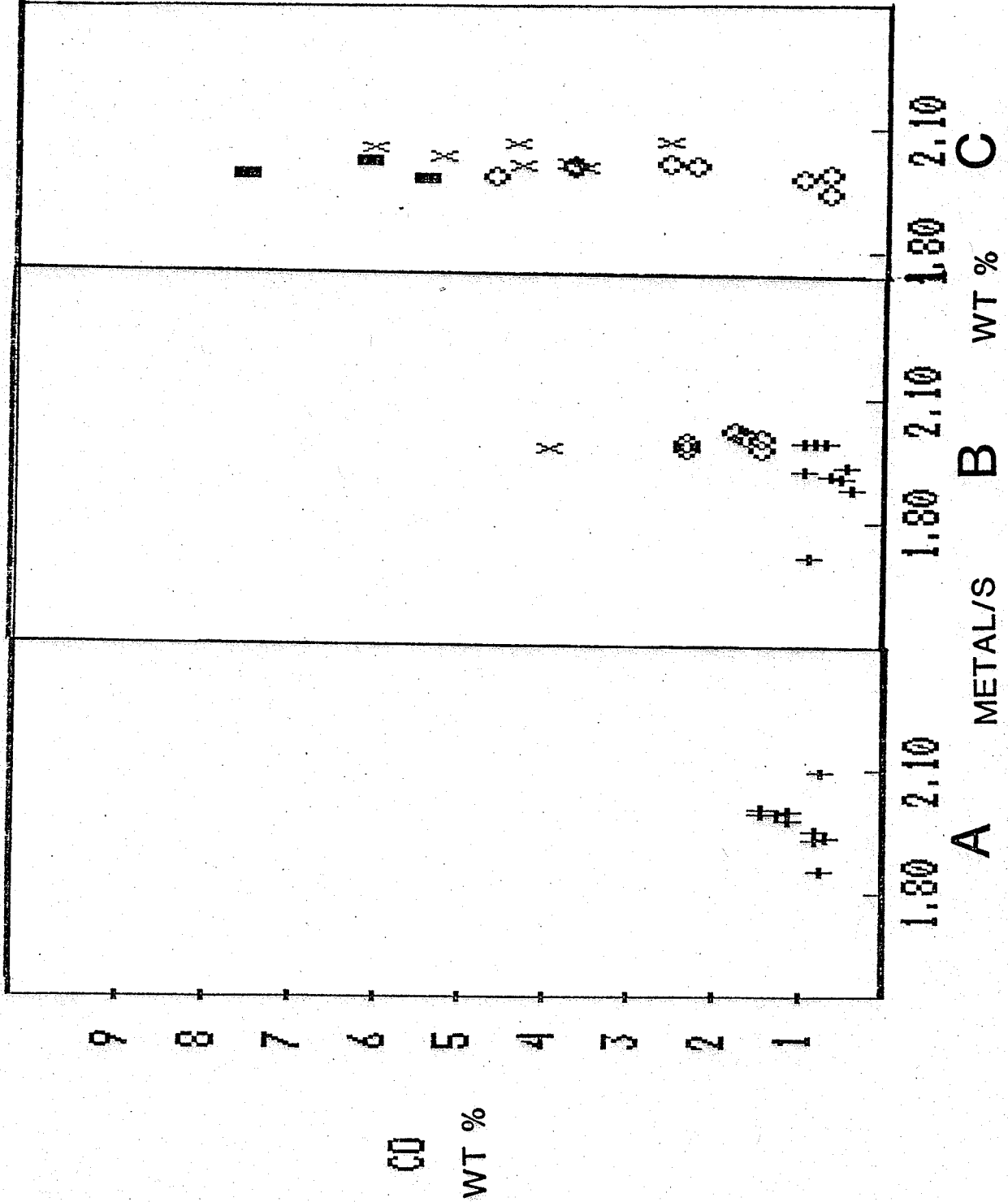


Fig. 6

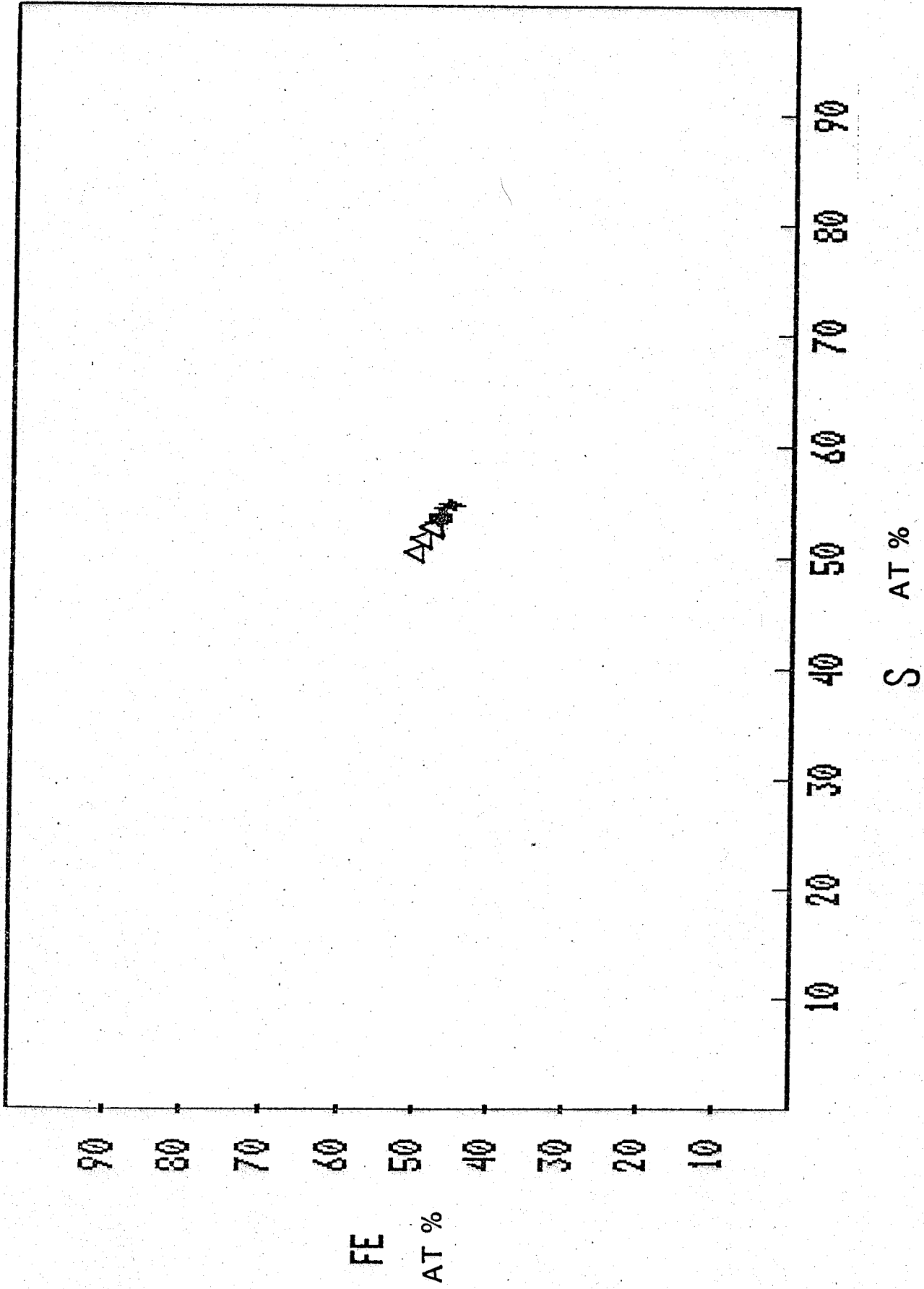
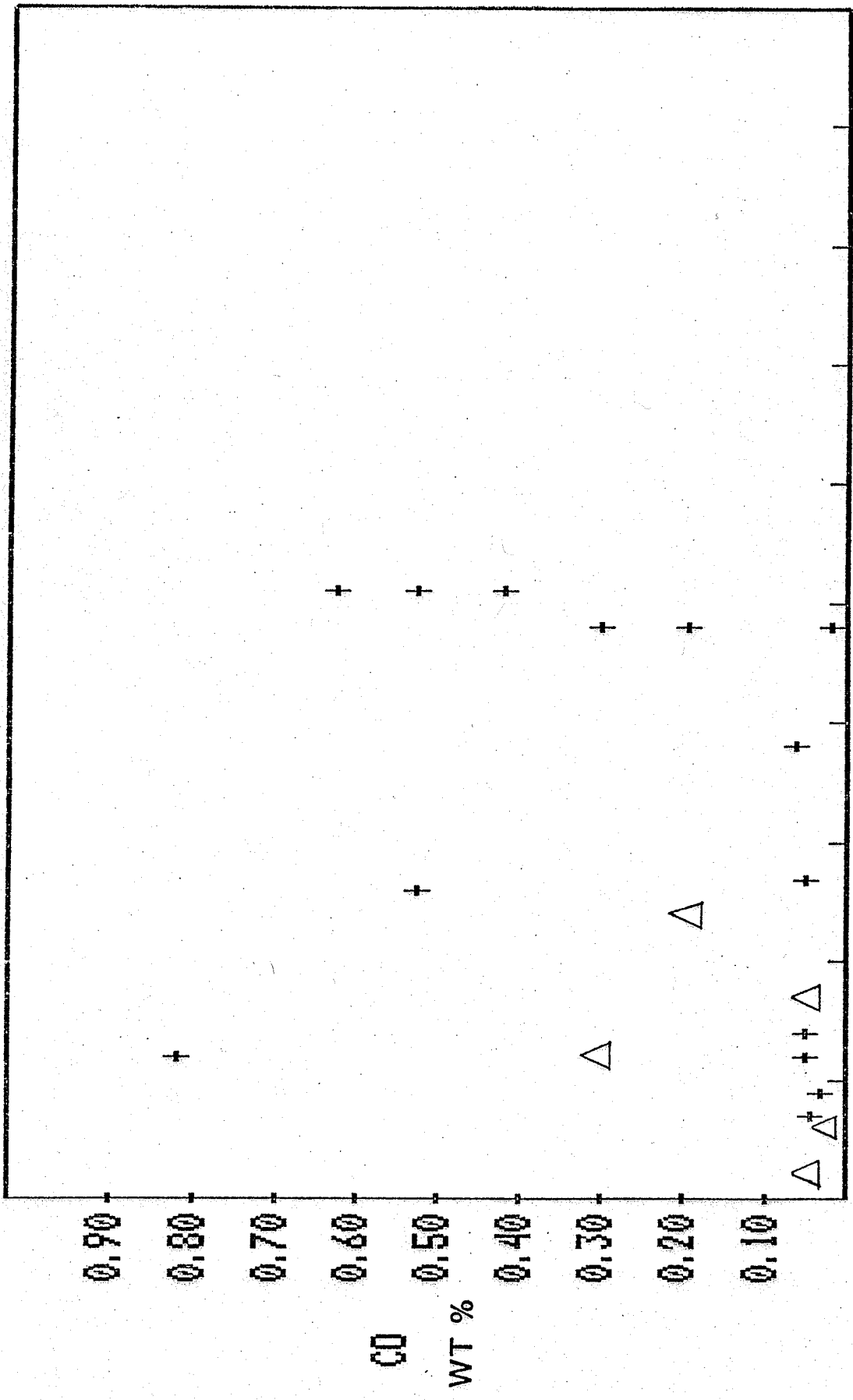


Fig. 7



NI WT %

Fig. 8

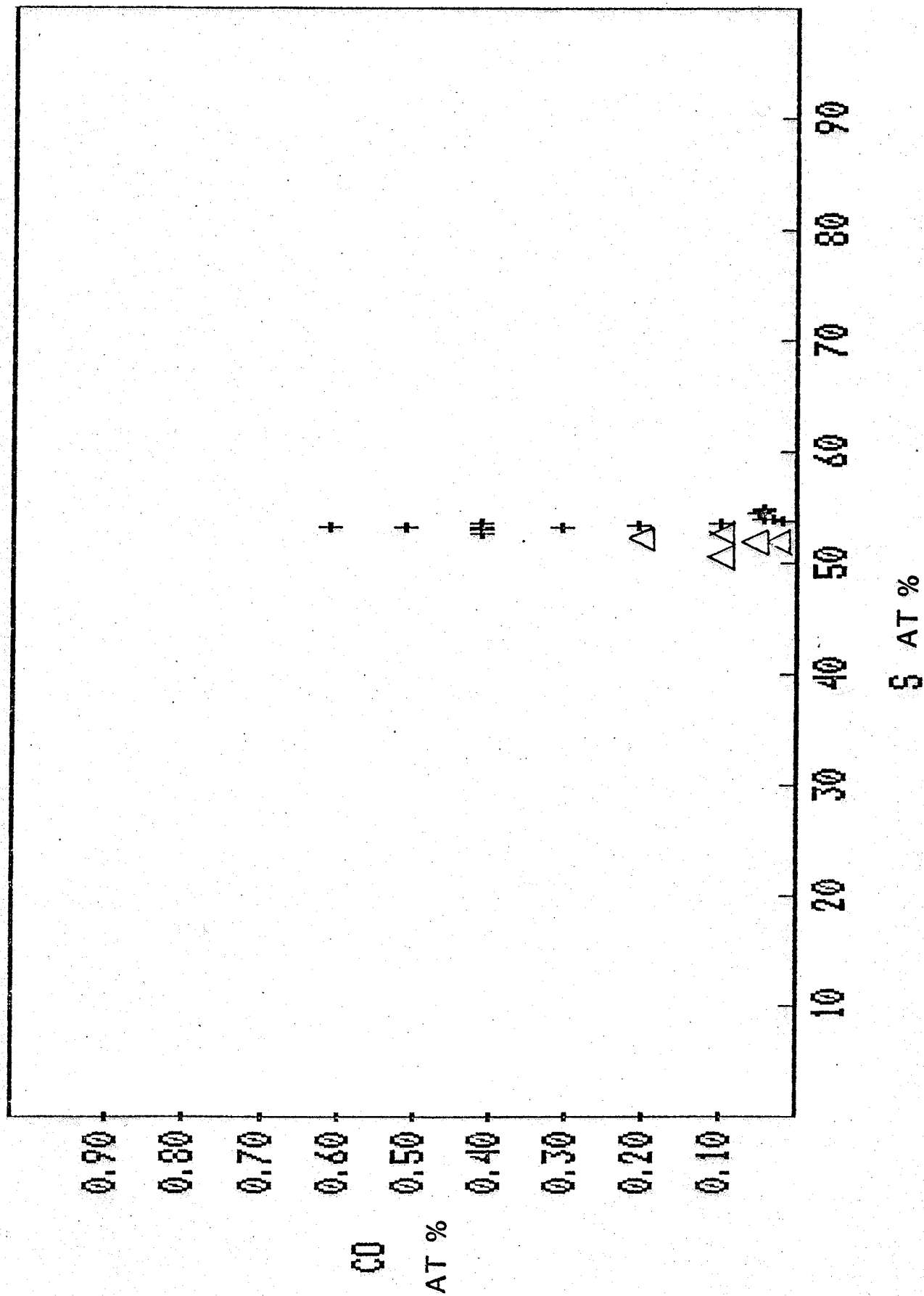


Fig. 9

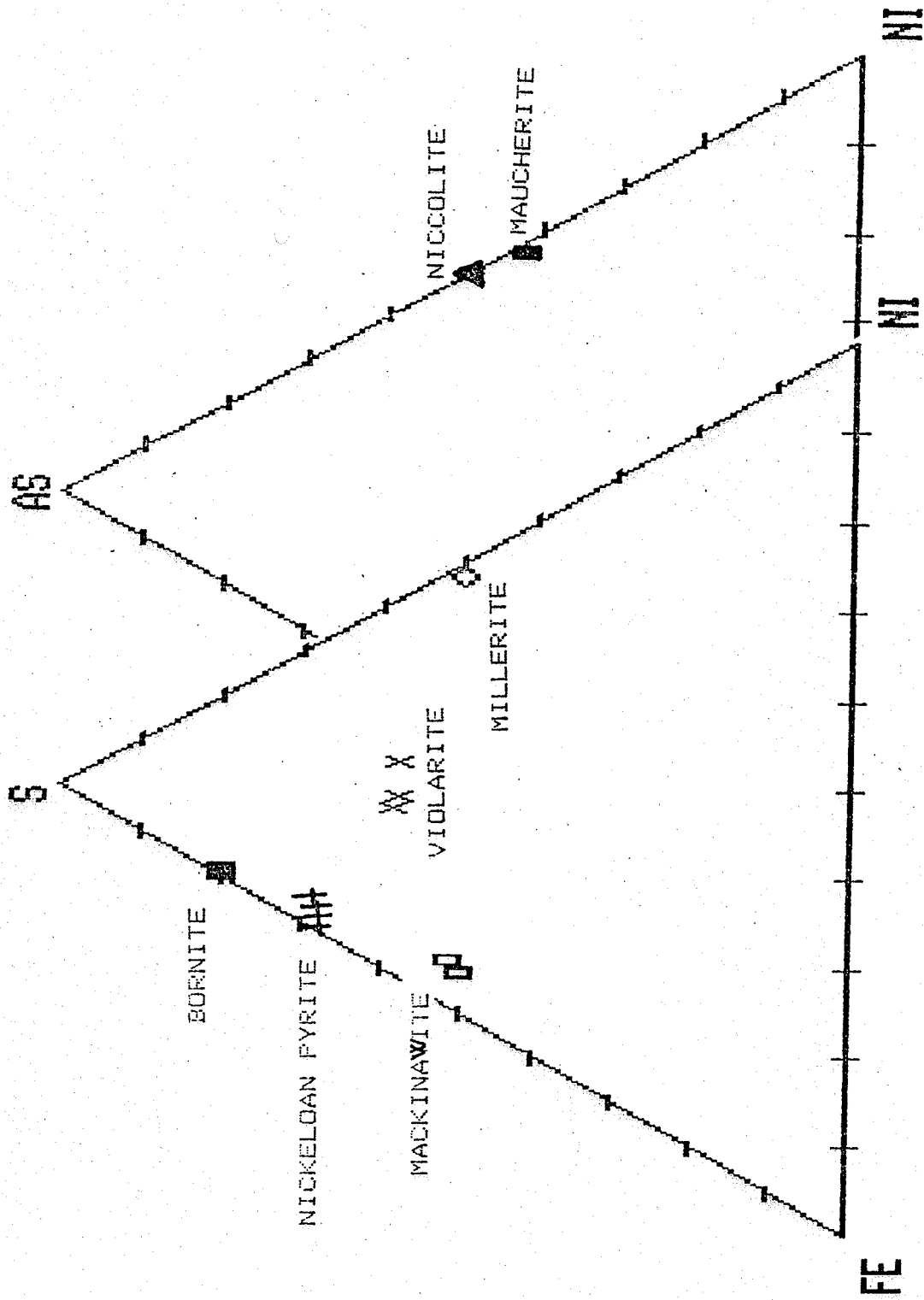
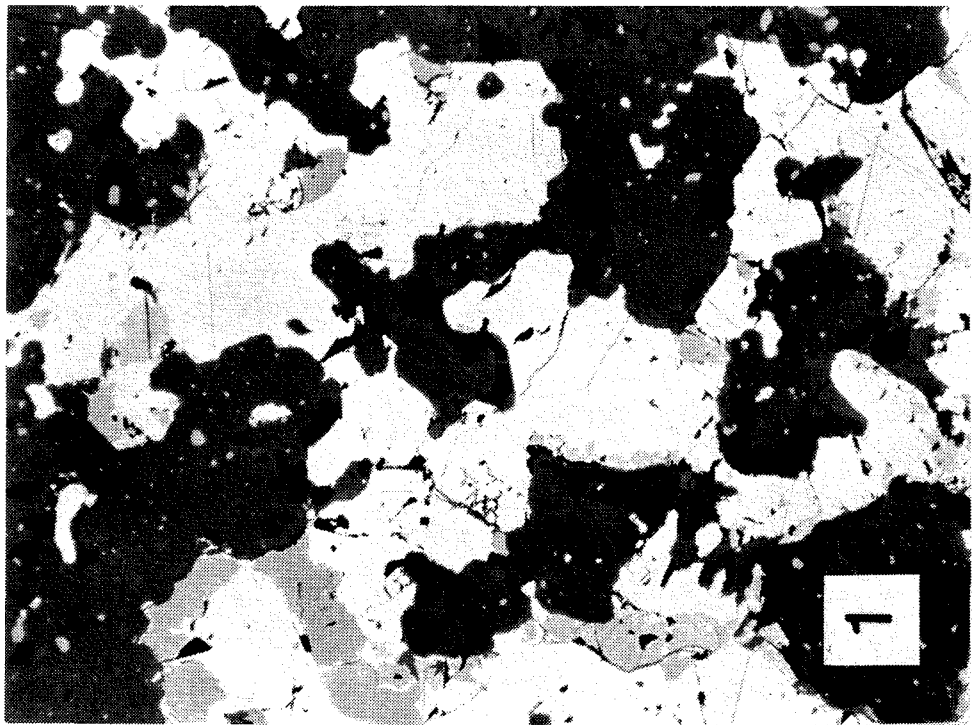
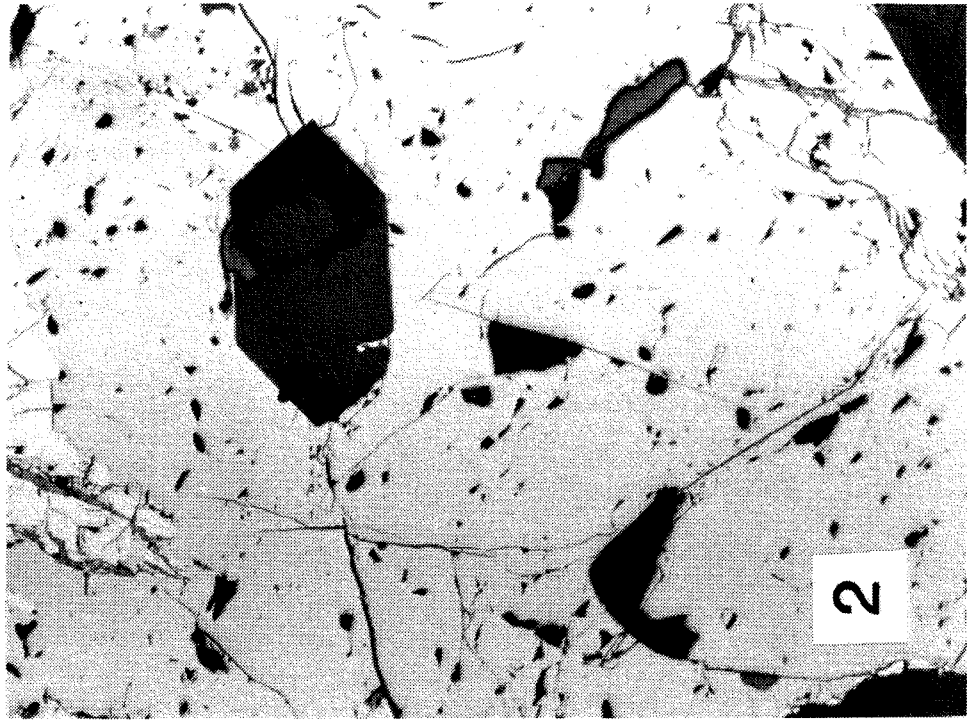
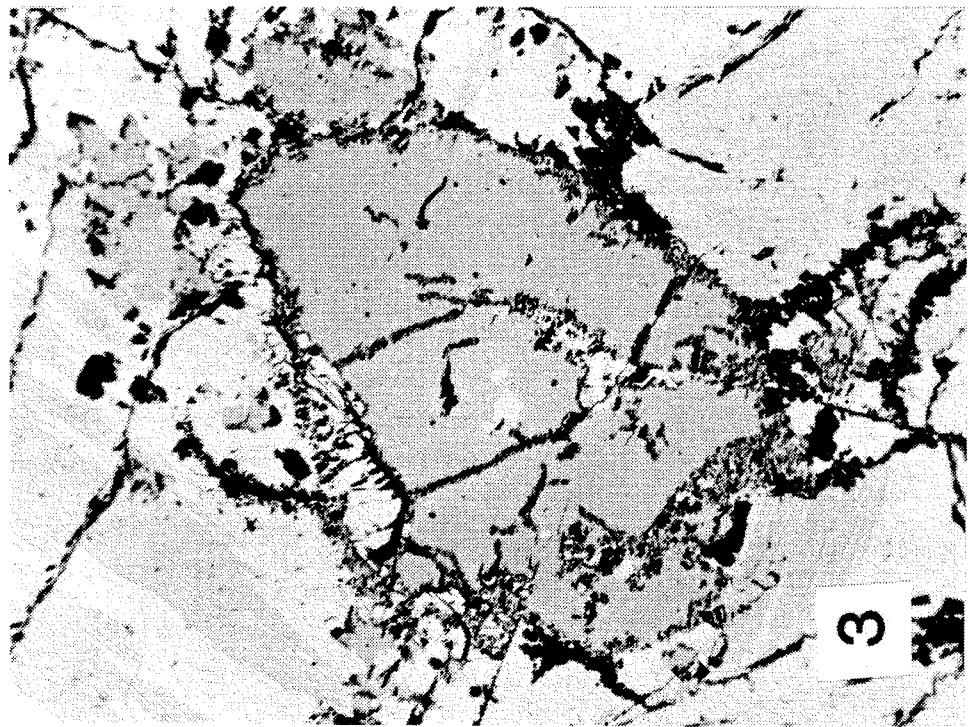
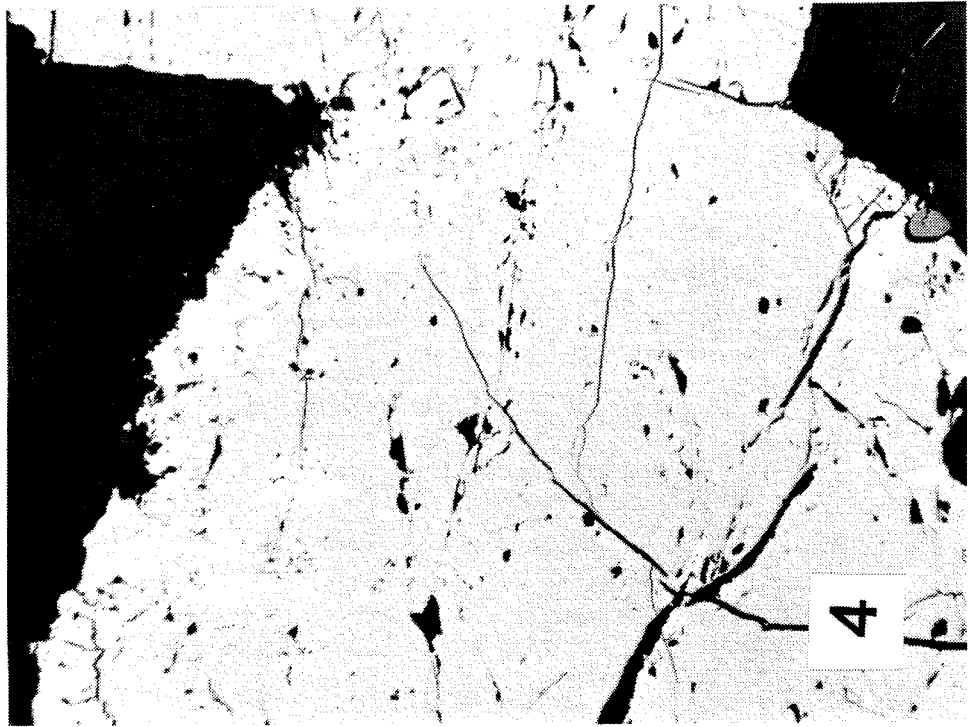
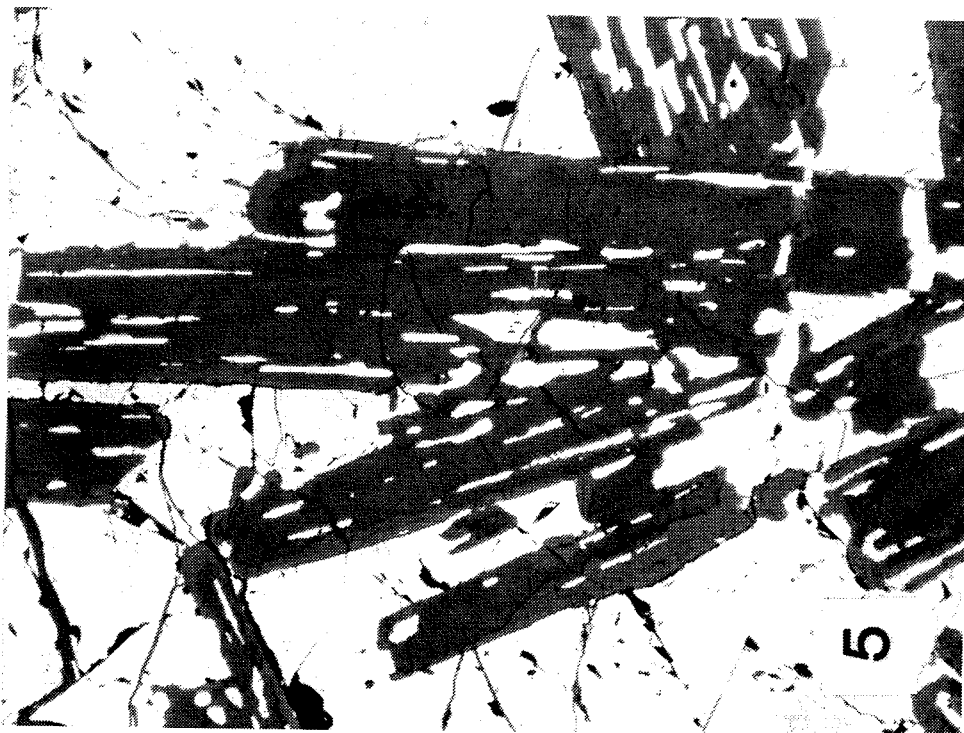
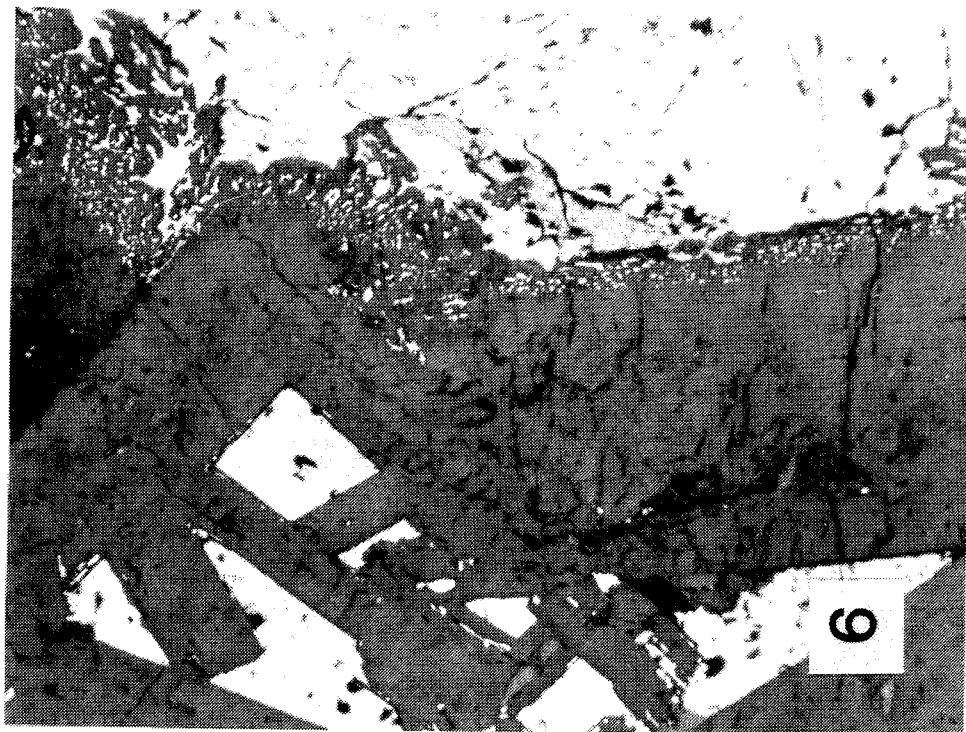


Fig. 10







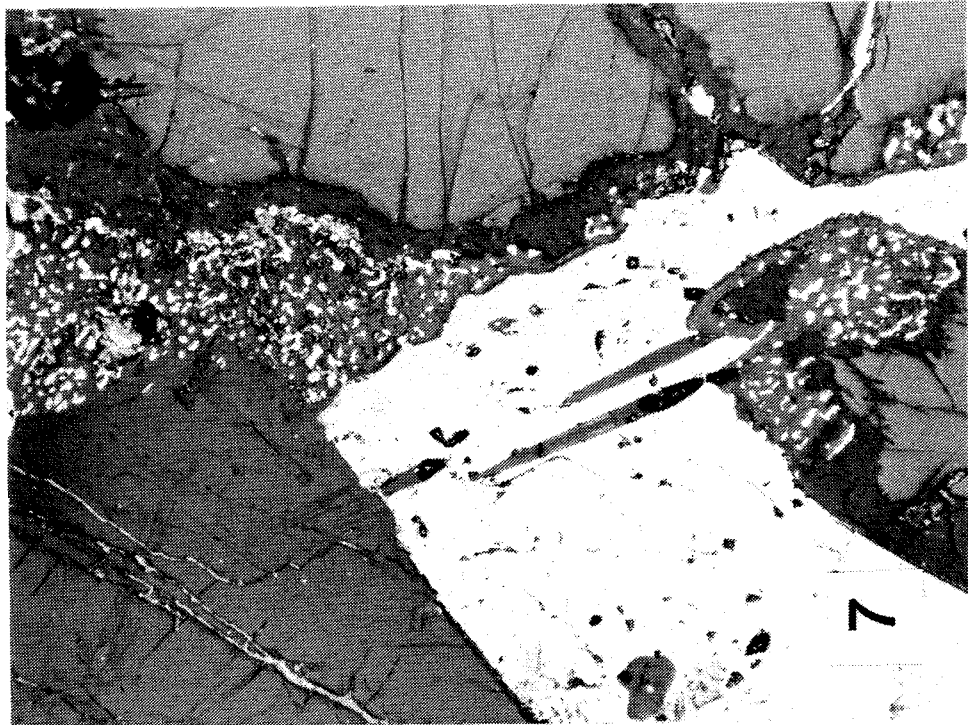
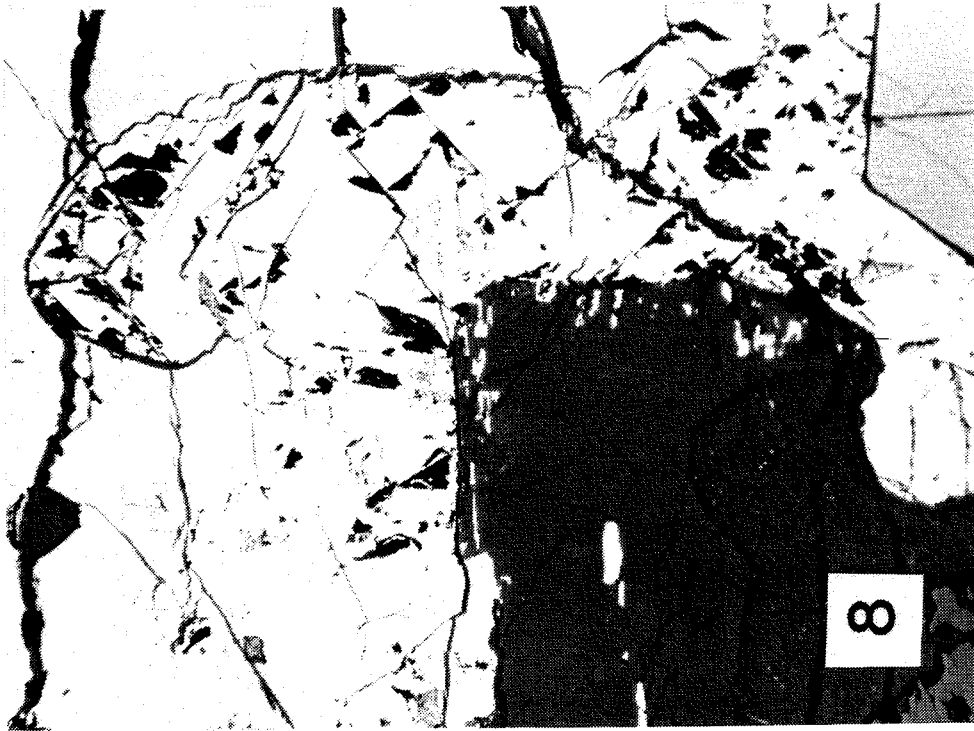


TABLE 1. ELECTRON MICROPROBE ANALYSES OF HEXAGONAL PYRRHOTITES

	1	2	3	4	5	6	7	8	9
FE2	61.53	60.44	60.80	60.85	61.97	60.30	60.62	60.42	60.29
CO	0.04	0.02	nd	0.04	0.06	0.03	0.19	0.29	nd
NI	0.02	0.06	nd	0.17	nd	nd	0.24	0.12	0.85
CU	nd	0.02	nd	0.05	0.16	nd	nd	nd	0.12
S	38.09	37.63	37.25	37.11	38.05	37.21	39.02	38.56	37.94
TOTAL	99.68	98.17	98.05	98.20	100.24	97.54	100.07	99.39	99.20
ATOM %									
S	51.79	51.92	51.57	51.36	51.53	51.74	52.70	52.50	51.90
FE2	48.04	47.88	48.32	48.35	48.18	48.13	47.00	47.20	47.40
CO	0.03	0.02	nd	0.03	0.05	0.03	0.10	0.20	nd
NI	0.02	0.05	nd	0.01	nd	nd	0.20	0.10	0.60
CU	nd	0.02	nd	nd	0.10	nd	nd	nd	0.10

- 1 - CYCLIC ZONE GABBRO 254/1-1-5
- 2 - CYCLIC ZONE GABBRO 130/3-1-4
- 3 - CYCLIC ZONE GABBRO 130/3-2-10
- 4 - CYCLIC ZONE FINE GRAINED GABBRO 258/2-1-3
- 5 - CYCLIC ZONE GABBRO 160/1-2-10
- 6 - CYCLIC ZONE GABBRO 430C-2-4
- 7 - MINERALIZED ZONE GABBRO DH18-160-7-3
- 8 - MINERALIZED ZONE GABBRO 141/1531-4-7
- 9 - FELSIC VEIN IN HORNFELS-CONTACT ZONE 303/2625-2-7

TABLE 2. ELECTRON MICROPROBE ANALYSES OF MONOCLINIC PYRRHOTITES.
PAGE 1

	1	2	3	4	5	6	7	8	9	10	11	12
S	40.07	39.17	39.41	39.38	39.75	40.96	39.90	39.87	39.96	39.30	39.45	39.46
FE2	59.39	58.28	58.46	58.48	60.22	59.36	59.39	55.63	56.45	58.79	59.12	59.44
CO	0.02	0.03	0.05	0.04	0.51	nd	0.19	0.05	0.05	0.80	0.29	0.41
NI	0.48	0.09	0.12	0.07	0.51	0.36	0.48	0.14	0.27	0.12	0.48	0.51
CU	0.03	nd	nd	nd	0.16	nd	0.16	2.04	0.58	0.50	nd	0.16
TOTAL	99.69	97.57	98.04	98.97	101.15	100.68	100.12	98.73	97.55	99.51	99.34	99.98

ATOM. %

S	53.77	53.84	53.89	53.89	53.00	54.40	53.60	54.57	54.78	53.20	53.40	53.20
FE	45.76	45.98	45.90	45.95	46.10	45.30	45.80	43.71	44.44	45.80	46.00	46.00
CO	0.02	0.03	0.04	0.03	0.40	nd	0.10	0.04	0.04	0.60	0.20	0.30
NI	0.35	0.07	0.10	0.06	0.40	0.30	0.40	0.10	0.21	0.10	0.40	0.40
CU	0.03	nd	nd	nd	0.10	nd	0.10	1.40	0.40	0.30	nd	0.10

- 1 - CYCLIC ZONE GABBRO 254/1-1-7
- 2 - CYCLIC ZONE GABBRO 130/3-2-9
- 3 - CYCLIC ZONE GABBRO 300/1387-3B-5
- 4 - CYCLIC ZONE GABBRO 300/1387-3A-11
- 5 - MINERALIZED ZONE GABBRO 300/1767-4-3
- 6 - MINERALIZED ZONE GABBRO 18/30-1-12
- 7 - MINERALIZED ZONE GABBRO 18/30-2-5
- 8 - MINER. ZONE PEGM. PYRRHOTITE LAMELLAE IN CUBANITE 18/10-1-6
- 9 - MINER. ZONE PEGM. PYRRHOTITE LAMELLAE IN CUBANITE 18/10-1-7
- 10 - MINER. ZONE PEGM. PYRRHOTITE LAMELLAE IN CUBANITE 18/10-8-8
- 11 - MINERALIZED ZONE XENOLITH 141/1426-1-5
- 12 - MINERALIZED ZONE XENOLITH 300/1450-1-3

TABLE 2. MONOCLINIC PYRRHOTITES. PAGE 2.

	13	14	15	16	17
S	40.19	39.72	39.72	38.84	39.09
FE2	58.17	59.74	59.14	59.64	59.11
CO	0.06	0.51	0.51	0.61	0.61
NI	0.38	0.26	0.51	0.51	nd
CU	nd	nd	nd	nd	nd
TOTAL	98.93	100.37	99.88	99.60	98.81
	ATOM. %				
S	54.39	53.30	53.50	52.70	53.20
FE	45.21	46.00	45.70	46.50	46.30
CO	0.05	0.40	0.40	0.40	0.50
NI	0.28	0.20	0.40	0.40	nd
CU	nd	nd	nd	nd	nd

- 13 - MINERALIZED ZONE XENOLITH 303/2181-5-1
- 14 - MINERALIZED ZONE XENOLITH 303/2181-2-5
- 15 - CONTACT ZONE HORNFELS 140/2480-1-8
- 16 - CONTACT ZONE HORNFELS 140/2542-2-4
- 17 - CONTACT ZONE HORNFELS 301/2620-1-2

TABLE 3. ELECTRON MICROPROBE ANALYSES OF PENTLANDITES ASSOCIATED WITH MONOCLINIC PYRRHOTITES. PAGE 1.

	1	2	3	4	5	6	7	8	9	10	11	12
S	33.46	33.55	34.01	33.15	33.45	33.80	33.30	33.32	33.38	33.67	33.44	32.90
FE	30.68	30.21	29.39	29.67	29.65	27.74	26.77	29.44	31.30	29.71	30.58	29.14
CO	0.98	0.65	0.65	2.49	2.19	7.38	5.98	5.28	3.58	3.59	4.49	3.68
NI	34.46	35.87	35.87	34.68	35.31	32.01	34.57	31.20	31.98	34.33	31.24	33.52
CU	0.32	nd	nd	0.16	0.16	nd	nd	nd	0.64	nd	nd	0.16
TOTAL	99.90	100.28	99.92	100.15	100.92	100.93	100.62	99.24	101.20	101.30	99.75	99.56
ATOM. %												
S	47.40	47.30	48.00	47.10	47.10	47.50	47.00	47.50	46.90	47.10	47.40	46.90
FE	25.00	24.50	23.80	24.10	23.90	22.40	21.70	24.10	25.20	23.90	24.90	23.90
CO	0.80	0.50	0.50	1.90	1.70	5.60	4.60	4.10	2.70	2.70	3.50	2.90
NI	26.60	27.70	27.70	26.80	27.10	24.50	26.70	24.30	24.50	26.30	24.20	26.10
CU	0.20	nd	nd	0.10	0.10	nd	nd	nd	0.50	nd	nd	0.10
FE+CO	31.66	30.86	30.04	32.16	31.84	35.12	32.75	34.72	34.88	33.30	35.07	32.82
NI+FE	66.12	66.73	65.91	66.84	67.15	67.13	67.32	65.92	66.86	67.63	66.31	66.34
NI/S	1.98	1.99	1.94	2.02	2.01	1.99	2.02	1.98	2.00	2.01	1.98	2.02

- 1- MINERALIZED ZONE PEGMATITE 18/10-8-13
- 2- MINERALIZED ZONE GABBRO 18/30-2-4
- 3- MINERALIZED ZONE GABBRO 18/30-1-10
- 4- MINERALIZED ZONE GABBRO 300/1767-4-1
- 5- MINERALIZED ZONE GABBRO 300/1767-1-7
- 6- MINERALIZED ZONE XENOLITH 141/1426-1-1
- 7- MINERALIZED ZONE XENOLITH 300/1450-1-2
- 8- MINERALIZED ZONE XENOLITH 303/2581-2-4
- 9- MINERALIZED ZONE GABBRO 300/2247-7-9
- 10- MINERALIZED ZONE GABBRO 300/2247-8-1
- 11- BASAL ZONE CONTACT GABBRO 303/2596-4-2
- 12- CONTACT ZONE HORNFELS 140/2480-1-6

TABLE 3. PENTLANDITES. PAGE 2.

	13	14	15	16	17
S	33.39	33.03	32.51	32.69	32.43
FE	29.65	29.18	29.79	30.59	29.97
CO	3.49	4.18	4.24	5.13	5.94
NI	33.70	33.04	32.98	30.71	30.61
CU	nd	nd	0.37	0.22	0.52
TOTAL	100.23	99.43	100.08	99.60	99.68
	ATOM. %				
S	47.20	47.20	46.30	46.70	46.40
FE	24.10	23.90	24.40	25.00	24.60
CO	2.70	3.20	3.30	4.00	4.60
NI	26.00	25.70	25.60	23.90	23.90
CU	nd	nd	0.30	0.20	0.40
FE+CO	33.14	33.36	34.03	35.72	35.91
NI+FE	66.84	66.40	67.01	66.43	66.52
NI/S	2.00	2.01	2.06	2.03	2.05

- 13 - CONTACT ZONE HORNFELS 140/2484-2-1
- 14 - CONTACT ZONE HORNFELS 140/2542-2-3
- 15 - BASAL ZONE HORNFELS 201/493-1-3
- 16 - BASAL ZONE HORNFELS 201/504-1-2
- 17 - CONTACT ZONE HORNFELS 201/525-1-1

TABLE 4. ELECTRON MICROPROBE ANALYSES OF PENTLANDITES ASSOCIATED WITH HEXAGONAL PYRRHOTITES. PAGE 1.

	1	2	3	4	5	6	7	8	9	10	11	12
S	35.32	36.78	34.60	33.51	34.93	33.90	33.17	33.22	33.22	32.86	33.15	33.40
FE	33.94	29.99	32.42	35.58	34.19	32.59	34.64	32.02	30.88	30.57	33.08	33.06
CO	0.37	0.84	0.93	0.80	0.49	0.45	0.65	0.93	1.40	1.68	1.58	1.40
NI	32.05	32.23	33.11	30.41	31.96	32.60	30.84	33.22	34.35	34.09	31.95	31.50
CU	0.05	0.45	0.01	0.16	nd	0.42	nd	0.15	nd	nd	0.15	nd
TOTAL	101.82	100.47	101.19	100.62	101.79	100.11	99.30	99.54	99.85	99.20	99.91	99.36
	ATOM. %											
S	48.58	50.83	48.15	47.20	48.27	47.79	47.20	47.30	47.10	47.00	47.10	47.40
FE	26.87	23.80	25.90	28.70	27.12	26.38	28.30	26.10	25.20	25.10	26.90	27.00
CO	0.28	0.64	0.70	0.60	0.37	0.35	0.50	0.70	1.10	1.30	1.20	1.10
NI	24.14	24.32	25.17	23.30	24.12	25.10	24.00	25.80	26.60	26.60	24.70	24.50
CU	0.04	0.32	0.01	0.10	nd	0.30	nd	0.10	nd	nd	0.10	nd
FE+CO	34.31	30.83	33.35	36.38	34.68	33.04	35.29	32.95	32.28	32.25	34.66	34.46
NI+FE	66.36	63.06	66.46	66.79	66.64	65.64	66.13	66.17	66.63	66.34	66.61	65.96
NI/S	1.88	1.71	1.92	1.99	1.91	1.94	1.99	1.99	2.01	2.02	2.01	1.97

- 1- CYCLIC ZONE GABBRO 254/1-1-2
- 2- CYCLIC ZONE GABBRO 130/3-1-1
- 3- CYCLIC ZONE GABBRO 130/3-1-8
- 4- CYCLIC ZONE GABBRO 268/1-1-11
- 5- CYCLIC ZONE GABBRO 160/1-1-6
- 6- CYCLIC ZONE GABBRO 258/2-1-5
- 7- CYCLIC ZONE GABBRO 300/1387-3-7
- 8- CYCLIC ZONE GABBRO 141/812-1-3
- 9- MINERALIZED ZONE GABBRO DH18-160-7-6
- 10- MINERALIZED ZONE GABBRO DH18-160-8-1
- 11- MINERALIZED ZONE GABBRO 141/1130-1-3
- 12- MINERALIZED ZONE GABBRO 141/1130-5-1

TABLE 4. PENTLANDITES. PAGE 2.

	13	14	15
S	33.50	32.88	33.58
FE	32.59	32.19	33.01
CO	2.24	2.24	3.83
NI	31.36	31.09	29.60
CU	0.15	nd	0.19
TOTAL	99.84	98.40	100.21
	ATOM. %		
S	47.50	47.20	47.30
FE	26.50	26.60	26.80
CO	1.70	1.80	2.90
NI	24.20	24.40	22.80
CU	0.10	nd	0.10
FE+CO	34.83	34.43	36.84
NI+FE	66.19	65.52	66.44
NI/S	1.98	1.99	1.98

13 - MINERALIZED ZONE GABBRO 141/1531-4-3

14 - MINERALIZED ZONE GABBRO 141/1531-5-2

15 - FELSIC VEIN IN HORNFELS-CONTACT ZONE 303/2625-2-5

TABLE 5. ELECTRON MICROPROBE ANALYSES OF PENTLANDITES ASSOCIATED WITH CHALCOPYRITE

	1	2	3	4	5	6	7	8	9	10
S	34.72	34.96	34.63	33.70	33.44	33.42	33.46	33.27	32.27	34.13
FE	27.96	30.01	29.70	27.58	26.68	26.97	27.52	28.68	28.89	28.25
CO	0.71	0.82	0.77	1.09	1.19	1.09	1.39	1.40	0.76	0.68
NI	35.73	36.57	37.01	38.62	38.69	37.97	37.85	36.61	37.94	37.08
CU	0.20	0.27	0.28	0.16	0.32	0.16	0.32	0.15	0.18	0.17
TOTAL	99.49	102.83	102.60	101.15	100.48	99.61	100.70	100.11	100.04	100.57
ATOM. %										
S	49.00	48.00	47.73	47.30	47.30	47.60	47.20	47.20	46.00	47.95
FE	22.66	23.66	23.50	22.20	21.60	22.00	22.30	23.30	23.70	22.79
CO	0.55	0.61	0.58	0.80	0.90	0.80	1.10	1.10	0.60	0.52
NI	27.54	27.43	27.86	29.60	29.90	29.50	29.10	28.30	29.60	28.46
CU	0.15	0.19	0.20	0.10	0.20	0.10	0.20	0.10	0.10	0.12
FE+CO	28.67	30.83	30.47	28.67	27.87	28.06	28.91	30.08	29.65	28.93
NI+FE	64.40	67.40	67.48	67.29	66.56	66.03	66.76	66.69	67.59	66.01
NI/S	1.85	1.93	1.95	2.00	1.99	1.98	2.00	2.00	2.09	1.93

- 1 - CYCLIC ZONE GABBRO 160/1-1-1
- 2 - CYCLIC ZONE GABBRO 160/1-1-2
- 3 - CYCLIC ZONE GABBRO 160/1-1-3
- 4 - CYCLIC ZONE GABBRO 268/1-4-1
- 5 - CYCLIC ZONE GABBRO 268/1-4-2
- 6 - CYCLIC ZONE GABBRO 268/1-4-3
- 7 - CYCLIC ZONE GABBRO 268/1-5-3
- 8 - CYCLIC ZONE GABBRO 141/812-11B-1
- 9 - MINERALIZED ZONE GABBRO 212/419-6-4
- 10 - MINER ZONE PEGM-PENT IN CB 18/10-1-4

TABLE 6. ELECTRON MICROPROBE ANALYSES OF PENTLANDITES ASSOCIATED WITH TROILITE

	1	2	3	4	5	6	7	8
S	33.07	33.61	34.24	33.27	32.53	32.31	32.13	32.12
FE	35.92	38.99	40.18	36.75	36.41	37.96	39.48	39.08
CO	0.36	0.55	0.55	0.47	0.56	0.34	0.40	0.31
NI	29.15	26.93	25.64	29.61	29.09	28.36	27.09	27.48
CU	nd	nd	0.16	nd	0.15	0.24	0.22	0.35
TOTAL	98.50	100.08	100.77	100.10	98.74	99.21	99.32	99.34
	ATOM. %							
S	47.40	47.40	47.80	47.00	46.70	46.20	45.90	45.90
FE	29.50	31.50	32.20	29.80	30.00	31.10	32.40	32.00
CO	0.30	0.40	0.40	0.40	0.40	0.30	0.30	0.20
NI	22.80	20.70	19.50	22.80	22.80	22.10	21.20	21.40
CU	nd	nd	0.10	nd	0.10	0.20	0.20	0.30

- 1 - SLUMPED FINE GRAINED GABBRO 258A-1A-6A
- 2 - SLUMPED FINE GRAINED GABBRO 258A-3-6A
- 3 - SLUMPED FINE GRAINED GABBRO 258A-3-7
- 4 - SLUMPED FINE GRAINED GABBRO 258B-1A-1
- 5 - SLUMPED FINE GRAINED GABBRO 258B-1A-5
- 6 - SLUMPED FINE GRAINED GABBRO 258B-1B-2
- 7 - SLUMPED FINE GRAINED GABBRO 258B-10-2
- 8 - SLUMPED FINE GRAINED GABBRO 258B-10-4

TABLE 7. ELECTRON MICROPROBE ANALYSES OF TROILITES

	1	2	3	4	5	6
S	36.29	37.14	35.51	35.51	35.82	34.74
FE	63.33	64.50	62.43	65.05	64.94	63.90
CO	nd	nd	nd	nd	0.07	nd
NI	nd	nd	0.12	0.04	0.30	nd
CU	nd	0.33	nd	nd	0.34	0.09
TOTAL	99.62	101.97	98.06	100.56	101.80	98.97

ATOM. %

	1	2	3	4	5	6
S	50.00	50.00	49.70	48.60	48.60	48.50
FE	50.00	49.80	50.20	51.20	50.70	51.20
CO	nd	nd	nd	nd	0.00	nd
NI	nd	nd	nd	nd	0.20	nd
CU	nd	0.20	nd	nd	0.20	0.10

- 1 - SLUMPED FINE GRAINED GABBRO CYCLE 2 258A-2-1
- 2 - SLUMPED FINE GRAINED GABBRO CYCLE 2 258A-1-7
- 3 - SLUMPED FINE GRAINED GABBRO CYCLE 2 258B-1A-4
- 4 - SLUMPED FINE GRAINED GABBRO CYCLE 2 258B-1A-2
- 5 - SLUMPED FINE GRAINED GABBRO CYCLE 2 258B-1A-7
- 6 - SLUMPED FINE GRAINED GABBRO CYCLE 2 258B-10-1

TABLE 8. ELECTRON MICROPROBE ANALYSES OF CHALCOPYRITES AND CUBANITES

	1	2	3	4	5	6
S	36.19	34.66	36.01	34.73	36.65	36.62
FE	29.40	30.75	28.56	30.26	40.12	38.94
CO	nd	nd	0.03	nd	0.30	0.04
NI	0.05	nd	0.02	nd	nd	0.02
CU	34.64	33.87	34.99	34.59	23.93	23.78
TOTAL	100.40	99.50	99.94	99.58	101.00	99.64
	ATOM. %					
S	51.23	49.86	51.27	49.90	50.98	51.19
FE	23.89	25.40	23.35	25.00	32.04	31.14
CO	nd	nd	0.03	nd	0.02	0.03
NI	0.04	nd	0.02	nd	nd	0.02
CU	24.75	24.59	25.14	25.10	16.80	16.88

- 1 - CHALCOPYRITE, CYCLIC ZONE GABBRO 430C-1-3
- 2 - CHALCOPYRITE, CYCLIC ZONE GABBRO 130/2-1-1
- 3 - CHALCOPYRITE, MINER. ZONE PEGMATITE DH18/10-1-1
- 4 - CHALCOPYRITE, CONTACT ZONE HORNFELS 201/525-1-4
- 5 - CUBANITE, CYCLIC ZONE GABBRO 160/1-2-11
- 6 - CUBANITE, MINER. ZONE PEGMATITE DH18/10-1-5

TABLE 9. ELECTRON MICROPROBE ANALYSES OF VIOLARITES, MACKINAVITES,
BORNITES AND MILLERITES

	1	2	3	4	5	6	7	8	9
S	41.91	42.72	42.20	35.77	36.11	37.11	26.21	26.20	35.47
FE	28.60	29.32	23.39	57.98	57.51	54.91	11.41	11.13	1.61
CO	0.55	0.50	1.08	0.41	0.43	0.40	0.16	0.16	0.30
NI	27.24	24.69	32.07	5.92	6.02	6.51	0.11	0.57	63.56
CU	nd	nd	0.03	0.08	0.09	0.68	63.47	61.50	0.31
TOTAL	98.43	97.39	98.88	100.30	100.36	99.91	101.36	99.56	101.25
					ATOM. %				
S	56.97	58.22	57.19	49.26	49.61	50.92	40.40	40.80	49.70
FE	22.33	22.94	18.20	45.83	45.36	43.25	10.10	9.90	1.30
CO	0.41	0.38	0.80	0.31	0.32	0.30	0.10	0.10	0.20
NI	20.23	18.38	23.74	4.45	4.52	4.88	0.10	0.50	48.60
CU	nd	nd	0.02	0.06	0.06	0.47	49.30	48.30	0.20

- 1 - VIOLARITE CYCLIC ZONE GABBRO 160/1-2-8
- 2 - VIOLARITE CYCLIC ZONE GABBRO 160/1-2-7
- 3 - VIOLARITE CYCLIC ZONE GABBRO 130/3-1-7
- 4 - MACKINAVITE CYCLIC ZONE GABBRO 130/2
- 5 - MACKINAVITE CYCLIC ZONE GABBRO 130/2
- 6 - MACKINAVITE MINERALIZED ZONE GABBRO 18/80-1-1A
- 7 - BORNITE CYCLIC ZONE GABBRO 245/4-8-22
- 8 - BORNITE CYCLIC ZONE GABBRO 255/1-7-5
- 9 - MILLERITE MINERALIZED ZONE 140/2415-5-210

TABLE 10. ELECTRON MICROPROBE ANALYSES OF NICKELOAN PYRITES, PYRITES,
AND NICKELOAN MARCASSITES

	1	2	3	4	5	6	7	8	9	10
S	54.24	52.60	53.08	52.70	53.19	53.16	52.76	53.67	50.68	52.59
FE	45.24	37.76	39.56	39.68	43.36	41.86	44.96	46.05	44.79	42.39
CO	0.73	0.93	0.31	0.93	0.52	0.42	0.31	0.42	0.21	0.41
NI	1.29	7.19	6.17	5.01	2.71	3.61	nd	nd	2.83	3.87
CU	nd	nd	nd	nd	nd	nd	nd	0.16	0.16	0.16
TOTAL	101.50	98.48	99.12	98.32	99.78	99.05	98.03	100.30	98.67	99.42
ATOM. %										
S	66.70	66.90	66.90	67.00	66.50	66.90	67.00	66.70	64.90	66.20
FE	31.90	27.50	28.60	28.90	31.20	30.30	32.80	32.90	32.90	30.70
CO	0.50	0.60	0.20	0.60	0.40	0.30	0.20	0.30	0.10	0.30
NI	0.90	5.00	4.30	3.50	1.90	2.50	nd	nd	2.00	2.70
CU	nd	nd	nd	nd	nd	nd	nd	0.10	0.10	0.10

1 - NICKELOAN PYRITE MINERALIZED ZONE 140/2462-1B-7

2 - NICKELOAN PYRITE MINERALIZED ZONE 303/2519-7-6

3 - NICKELOAN PYRITE CONTACT GABBRO 303/2602-1-10

4 - NICKELOAN PYRITE CONTACT GABBRO 303/2596-2-7

5 - NICKELOAN PYRITE MINERALIZED ZONE 140/2415-10-4

6 - NICKELOAN PYRITE MINERALIZED ZONE 140/2415-2-23

7 - PYRITE CONTACT GABBRO 303/2596-3-12

8 - PYRITE CONTACT ZONE HORNFELS 301/2620-1-1

9 - NICKELOAN MARCASSITE MINERALIZED ZONE 140/2462-3-3

10 - NICKELOAN MARCASSITE MINERALIZED ZONE 303/2596-4-3

TABLE 11. ELECTRON MICROPROBE ANALYSES OF NICCOLITE AND MAUCHERITE

	1	2
S	0.23	0.07
FE	0.46	0.85
CO	0.72	0.71
NI	42.53	49.39
CU	0.05	nd
ZN	0.04	0.08
AS	53.55	47.26
SB	2.11	1.69
TOTAL	99.73	100.09

	ATOM. %
S	0.49
FE	0.56
CO	0.83
NI	48.74
CU	.06000
ZN	.04000
AS	48.09

1 - NICCOLITE MINERALIZED ZONE 202/502-1-9
 2-MAUCHERITE MINERALIZED ZONE 202/502-2-14

